AGING AND DURABILITY OF HIGH TEMPERATURE ELECTRICAL INSULATION

GRANT NO. F496209510396

1 SEPT 1995-31 AUGUST 1999

FINAL REPORT

PROJECT MANAGER
DR. CHARLES Y-C LEE
AFOSR

PRINCIPAL INVESTIGATOR
CLARENCE J WOLF
WASHINGTON UNIVERSITY

REPORT DOCUMENTATION PAGE

AFRL-SR-BL-TR-00-

0155

1. AGENCY USE ONLY *(Leave blank)*	2. REPORT DATE	3. REPORT TYPE AND DATES COVERED
		FINAL 01 SEP 95 - 31 AUG 99

4. TITLE AND SUBTITLE
AGING AND DURABILITY OF HIGH TEMPERATURE ELECTRICAL INSULATION

5. FUNDING NUMBERS
F49620-95-1-0396

6. AUTHOR(S)
Clarence J Wolf

7. PERFORMING ORGANIZATION NAME(S) AND ADDRESS(ES)
Washington University
St Louis MO

8. PERFORMING ORGANIZATION REPORT NUMBER
F49620-95-1-0396

9. SPONSORING/MONITORING AGENCY NAME(S) AND ADDRESS(ES)
AFOSR/NL
801 N Randolph St., Rm 732
Arlington VA 22203-1977

10. SPONSORING/MONITORING AGENCY REPORT NUMBER

11. SUPPLEMENTARY NOTES

12a. DISTRIBUTION AVAILABILITY STATEMENT
Approved for public release; Distribution unlimited

12b. DISTRIBUTION CODE

13. ABSTRACT *(Maximum 200 words)*

The objectives of this program are to investigate the long-term aging processes which occur in typical high temperature polymeric systems. The primary system of interest is irradiated ethylene tetrafluorethylene (ETFE) coated over silver plated copper. The two specific goals of this research are: (1) To determine thermal oxidative degradation of a high temperaure polymer such as ETFE in the presence of metal surfaces, and (2) To determine the effect of the polymer on the overall stability and morphology of the metal surface. The kinetics of the ETFE degradation process as a function of radiation dose (used to cross-link the polymer, thereby enhancing its mechanical properties), temperature and catalytic metal surface were studies by several different thermal oxidative methods. Kinetic parameters, temperature coefficients (i.e., activation energies), and degradation rates as a function of temperature, radiation dose, and catalytic surfaces were investigated. Analytical procedures were used to determine the most accurate and reproducible method for kinetic analysis. The diffusion and subsequent surface reactions of copper through a thin silver plate (silver plated copper conductor) were studied by scanning Auger electron and optical spectroscopies. The kinetics of the copper diffusion are evaluated in order to correlate changes in the polymer degradation reactions with the change in surface chemistry and morphology of the metal. The initial silver surface slowly changes to an oxidized copper surface of the general stochiometry Cu 27 o as the copper diffuses through the silver layer. The diffusion is more rapid and the copper surface layer is thicker when the conductor is covered with polymer. In this case the ratio of copper to oxygen at the surface is approximatley 3:1. The solubility of

14. SUBJECT TERMS	15. NUMBER OF PAGES
	54
	16. PRICE CODE

17. SECURITY CLASSIFICATION OF REPORT	18. SECURITY CLASSIFICATION OF THIS PAGE	19. SECURITY CLASSIFICATION OF ABSTRACT	20. LIMITATION OF ABSTRACT
UNCLASS	UNCLASS	UNCLASS	

Aging and Durability of High Temperature Electrical Insulation
Grant No. F496209510396
(1 Sept 1995 - 31 Aug 1999)

Project Manager
Dr. Charles Y-C Lee
AFOSR

Clarence J. Wolf
Washington University
St. Louis, Mo

Executive Summary

The objectives of this program are to investigate the long-term aging processes which occur in typical high temperature polymeric systems. The primary system of interest is irradiated ethylene tetrafluorethylene (ETFE) coated over silver plated copper. The two specific goals of this research are:

- To determine thermal oxidative degradation of a high temperature polymer such as ETFE in the presence of metal surfaces, and
- To determine the effect of the polymer on the overall stability and morphology of the metal surface.

The kinetics of the ETFE degradation process as a function of radiation dose (used to cross-link the polymer, thereby enhancing its mechanical properties), temperature and catalytic metal surface were studied by several different thermal oxidative methods. Kinetic parameters, temperature coefficients (i.e. activation energies), and degradation rates as a function of temperature, radiation dose, and catalytic surfaces were investigated. Analytical procedures were used to determine the most accurate and reproducible method for kinetic analysis.

The diffusion and subsequent surface reactions of copper through a thin silver plate (silver plated copper conductor) were studied by scanning Auger electron and optical spectroscopies. The kinetics of the copper diffusion are evaluated in order to correlate changes in the polymer degradation reactions with the change in surface chemistry and morphology of the metal. The initial silver surface slowly changes to an oxidized copper surface of the general stochiometry $Cu_{2.7}O$ as the copper diffuses through the silver layer. The diffusion is more rapid and the copper surface layer is thicker when the conductor is covered with polymer. In this case the ratio of copper to oxygen at the surface is approximately 3:1.

The solubility of organic fluids, carbon disulfide and toluene into another model system, polyphenylene sulfide, was investigated. The effect of temperature, morphology and pre-sorption annealing on the transport process was studied.

Appendix I: Support Personnel

Graduate Students

Jonathan Elders
Dept of Chemical Engineering
Washington University
St. Louis, MO 63130

Chris Long
Dept of Chemical Engineering
Washington University
St. Louis, MO 63130

Other Researchers

1. Dan Waddill
Professor
Dept of Physics and Materials Science
University of Missouri - Rolla
Rolla, MO

2. Sean McKinney
Department of Material Sciences
University of Missouri - Rolla
Rolla, MO

3. Bernie Sunier
Department of Material Sciences
Washington University

4. Angela Aiduck (Graduated)
Department of Material Sciences
Washington University
St. Louis, MO 63130

5. Enrique Farfun (Graduated)
Department of Chemical Engineering
Washington University
St. Louis, MO 63130

5. Cynthia Chew
Department of Chemical Engineering
Washington University
St. Louis, MO 63130

6. Scott Hager (Graduated)
   Department of Chemical Engineering
   Washington University
   St. Louis, MO 63130

Appendix II: Publications

1. C.J. Wolf, H.J. Brandon, V.L. Young, K.L. Jerina and A.P. Srivastave, "Chemical, Physical and Mechanical Analysis of Explanted Breast Implants," *Immunology of Silicones*, M. Potter and N.R. Rose Eds., Springer Verlag, New York, 1996, p 25.

2. Wolf CJ, Brandon JH, Jerina KL, Young VL. "Long-Term Aging of Implanted Silicone/Silica Composite Breast Implants." Proceeding, Eleventh International Conference on Composite Materials, Gold Coast, Queensland, Australia: ed. M.L. Murray, p 467 (1998).

3. "Thermo-Oxidative Degradation of Ethylene-Tetrofluorethylene," J.P. Elders and C.J. Wolf, 3rd National Graduate Research Polymer conference, 21-24 June 1998, University of Akron Polymer chemistry Division (ACS), pp 9-15.

4. H.J. Brandon, C.J. Wolf, V.L. Young and K.L. Jerina. "Effect of Surgical Implantation on the Local Shell Properties of SILASTIC®II Silicone Gel Breast Implants," J. Biomatl. Sci. (Polym. Ed.) in press.

5. Brandon, HJ, Peters, W., Young, V.L, Jerina, K.L., Wolf, C.J., and M.W. Schorr, "Analysis of Two Dow Corning Breast Implants Removed After 28 Years of Implantation," *Aesthetic Surgery*, Jan/Feb, 1999.

6. Brandon, HJ, Young, V.L, Jerina, K.L. and Wolf, C.J, "Effect of Implantation Surgery on the Average Strength Properties of Silicone Gel Breast Implants," *Aesthetic Surgery*, May/June, 1999.

7. Brandon, HJ, Jerina, K.L., Wolf, C.J, and Young, V.L, "Ultimate Strength Properties of Control and Explanted SILASTIC®0 and SILASTIC®I Silicone Gel-Filled Breast Implant Shells," *Aesthetic Surgery Journal*, Sept/Oct., 1999.

8. Brandon, HJ, Jerina, K.L., Wolf, C.J, and Young, V.L, "Ultimate Strength Properties of Control and Explanted SILASTIC®II Silicone Gel Breast Implant Shells" *Aesthetic Surgery Journal*, Mar./Apr. 2000.

9. Brandon, HJ, Young, V.L, Jerina, K.L. and Wolf, C.J, "SEM Characterization of Surgical Instrument Damage to Breast Implants," Submitted to *Plastic and Reconstructive Surgery*.

Book Reviews for ACS (Appear in JACS)

1. Resins for Coatings: Chemistry, Properties and Applications. D. Stöye and W. Frectay (Hanser-Gardner: Cincinnati, 1996).

2. Hydrocarbon Resins, R. Mildenberg, G. Collin and M. Zander (Wiley-VXH; New York 1997).

Publication supported by AFOSF

1. Environmental Stress Deformation of Poly (ether ether ketone), A.P. Srivastour, N. Depke, and C.J. Wolf, J. of Appl. Polym. Sci. 66 725-731 (1997).

2. Thermo-Oxidative Degradation of Irradiated Ethylene Tetrafluorethylenes, in Oxidative Behavior of Materials in Thermal Analytical Techniques, Eds. A.T. Riga and G.H. Patterson STP 1326 ASTM, 1997 pp. 116-127.

3. Sorption Toluene into Low Temperature Annotated Polyphenylene Sulfide, Mo. J. Undergrad Chem. Res. 7 45-55 (1998/1999).

4. C. J. Wolf and C. Chew. "Sorption of Toluene in Polyphenylene Sulfide (PPS)," J. Polym. Sci. (Phys. Ed.) (submitted).

5. C.J. Wolf. "Sorption of Carbon Disulfide in Polyphenylene Sulfide (PPS)," J. Polym. Sci. (Phys. Ed.) (submitted.)

Aging and Durability of High Temperature Electrical Insulation
Grant No. F496209510396
(1 Sept 1995 - 31 Aug 1999)

Final Report

Clarence J. Wolf
Washington University
St. Louis, Mo

1.0 Summary

The primary objectives of this program are to determine the long-term aging processes which occur in typical high temperature polymeric systems. Of particular interest is a determination of the factors which control the long-term durability of electrical insulation systems. In a separate, but related series of experiments, we have shown that the primary mode of failure of fluorinated thermoplastic co-polymers used as electrical insulation is stress cracking. Furthermore, we have observed that the cracks can be directly correlated with the thermal degradation of the insulation. Other polymers exhibit a different critical mode of failure, for example the polyimide, pp' diphenylene oxide pyromellitimide (commercially sold by DuPont as Kapton®) cracks when stressed in the presence of water, i.e. stress hydrolysis. (1) The particular system of interest in this study is irradiated ethylene tetrafluoroethylene (ETFE) over silver plated copper. The two specific goals of this research are:

- To determine thermal oxidative degradation mechanism of high temperature polymer such as ETFE in the presence of metal surfaces, and
- To determine the effect of the polymer on the overall stability and morphology of the metal surface.

The kinetics of the ETFE degradation process as a function of radiation dose (cross-linked polymer), temperature and catalytic metal surface were studied by several different methods. Kinetic parameters, temperature coefficients (i.e. activation energies), and degradation rates as a function of temperature, radiation dose, and catalytic surfaces were investigated. A combination of physical analytical methods, including ATR-FTIR, TGA, DSC, and GC/MS were used to study the polymer.

The effect of the polymer on the metal surfaces and the subsequent surface reactions of copper through a thin silver plate (silver plated copper) were studied by scanning Auger and scanning electron microscopy (SEM). The initial silver surface slowly changes to an oxidized copper surface of the general stochiometry $Cu_{2.7}O$ as the copper diffuses through the silver layer. The new surface layer has a catalytic effect upon the decomposition of the overlaying polymer.

The diffusion and solubility of two penetrants, carbon disulfide and toluene, into polyphenylenesulfide (PPS) were investigated. PPS composite is a tough material presently used in the nose of commercial aircraft. The effects of temperature, morphology, and annealing on the transport process were investigated. The data suggest that the voids/channels (free volume) formed during solvent induced crystallized are smaller than 92Å^3 but larger than 49 Å^3 and may be the rate determining factor in the transport process.

2.0 Introduction

The use of polymers and polymeric materials in critical components of both military and commercial aerospace systems is expanding rapidly. These materials have outstanding physical and chemical properties and their full potential has not been utilized. One of the major limitations of these materials is a lack of knowledge about their long-term properties (durability) in a hostile environment. Thus, the determinations of their lifetime, or aging characteristics, is an area of immediate concern. The prediction of the aging process is particularly difficult for new materials designed for the harsh complex aerospace environment. The high level of sophistication of modern aircraft requires a deep understanding of the effects of the environment on the operating system. One of the major areas of concern is the electrical system of the aerospace vehicle. Recent tragedies suggest that electrical insulation particularly with regard to cracking and flaking, may be the Achilles heel of fly-by-wire aircraft.

The high level of sophistication in modern aircraft electronic systems requires long term protection from a harsh operating environment. Modern aircraft require miles of electrical wiring to connect the various aircraft components. For example, smaller Air Force aircraft, such as the F-15 Eagle or F-16 Falcon, require more than 100,000 feet (30,000 m) of electrical wiring. Due to the tight demands on space, weight, energy and maintenance cost in aircraft of this high degree of sophistication, the insulation must be lightweight, have excellent dielectric properties, and must maintain thermal stability at high temperatures for a long period of time.

In addition to the high temperature requirements, the wire system must remain flexible at all operating conditions. As a general class of compounds, thermoplastic

resins exhibit many desirable properties, and one such resin system, irradiated ethylenetetrafluoroethylene is presently being extensively used in aerospace wiring systems. This is an extremely complex system, consisting of a semi-crystalline thermoplastic resin which is irradiated with high-energy elections to enhance its mechanical properties; in addition it contains several additives to minimize oxidation and maximize flame resistance. This complex system is placed in direct contact with an active metal, the conductor (silver coated copper), and maintained at elevated temperature for long periods of time. Aerospace wiring systems have a design goal of 10,000 hours at 200°C! The aging of a wire system is a complex phenomenon in which an organic polymer is in direct contact with a metal surface, the conductor. Many electronic systems which utilize circuit boards encounter a similar problem, i.e. organic polymer in contact with an active metal surface for an extended time period at elevated temperature.

The ETFE system is of particular interest for two reasons:

1) it comprises the basic part of the new, so-called "hybrid," insulation of use on many modern Air Force and Navy aircraft, and

2) it is a semi-crystalline thermoplastic resin system which is cross-linked by electron irradiation.

Therefore, we have material which has great practical use, a "high temperature," semi-crystalline, cross-linked thermoplastic in direct contact with a silver/copper metal surface.

Since ETFE is a semi-crystalline thermoplastics resin, we extended our studies to another thermoplastic polymer, i.e. polyphenylenesulfide, PPS. PPS is also considered a high performance thermoplastic resin which has physical properties similar to

polyetheretherketone (PEEK). In fact PPS composite (E-glass fibers) is a candidate for use on the nose of the Airbus Industries A-340 commercial jet. The melting point of PPS is approximately 285°C and its T_g is approximately 85°C. PPS, like PEEK, can be obtained in either the amorphous or semi-crystalline state and exhibits solvent induced crystallization in the presence of a wide variety of solvents. We were particularly interested in the transport properties of the organic fluids, toluene and carbon disulfide, into PPS. Areas of particular concern were 1) solubility, 2)rates of sorption, 3) desorption, 4) diffusion coefficient, 5) solvent induced crystallinity, and 6) thermal treatment (annealing) prior to sorption.

Program Objectives: The overall objective of this program was to develop a basic understanding of the factors which determine the long-term stability, i.e. durability, of high performance thermoplastic resin systems. The program can be conveniently divided into two specific projects:

1) To determine the long-term effects, i.e. durability, on the overall properties of a complex thermoplastic resin system in contact with an active metal surface, and to consider the effect of each of the many processing variables on the stability of this material; and

2) Characterize the transport properties of organic liquids whose characteristics represent those encountered in a harsh airspace environment into a typical semi-crystalline thermoplastic resin.

One of the more important aspects of this program is concerned with the practical question: what is the effect of each component of a system on the durability of the other components. This aspect of the general question of material durability is usually

neglected. Most electronic systems used in high performance systems consist of integrated circuits in which the various components are fabricated directly onto a circuit board. Normally the circuit board is an organic film, such as an epoxy or polyimide. The long-term stability and overall synergistic effect of the various components *on each other* is of direct relevance to this study.

3.0 Experimental

The terminology used in this report concerning the durability of the electrical insulation is as follows:

- Polymer and insulation are used interchangeably as the coating over a metal or conductor
- Conductor is silver plated copper
- Metal refers to the base metal
- Wire refers to a conductor coated with insulation.

Materials: The ETFE was commercial grade polymer containing approximately 2.5 –4% triallylisocyanurate (TIAC) cross-linking agent. The conductor was extrusion coated with polymer to form the wire and it was irradiated with 1.5 MeV electrons to specified doses. The nominal conductor was 19-strand silver-plated copper. Each strand is 0.15 mm in diameter, plated with a silver layer $5x10^{-5}$ cm thick. The data is summarized in Table 1.

Samples of 0.25 mm thick films of amorphous PPS (<1% crystallinity Ryton®) were obtained from the Phillips Chemical Co., (Bartlesville OK). They were dried in a vacuum oven at various temperatures ranging from 40°C to 110°C for 16 hours. Selected samples were crystallized at 120°C.

Thermo-oxidative Aging: Samples were aged for a specific time at temperatures ranging from 150°C to 300°C in a Precision Scientific Mechanical Convection oven 625. All samples were run in triplicate. The individual samples were weighed at selected

times and a weight loss versus time curve was established for all wires and insulation. The ambient atmosphere is limited to air.

Thermogravimetric analysis (TGA): A Thermal Analysis TA-2950 TGA equipped with an automatic sample inlet was used for all TGA analysis. The analyses were conducted in either air, nitrogen or oxygen at a flow rate of 60 cm^3/min. Isothermal, dynamic, and "thermal jump" methods were used to evaluate degradation rates. Each method determines different components of the kinetics "puzzle", including activation energy (which properly should be called temperature coefficient), rate, order, and mechanism. Dynamic TGA can be used as a multi-experimental method to determine activation energies, as shown by Flynn and Wall (2). Samples are degraded at a series of heating rates, and in each experiment, the temperature to reach a designated conversion is recorded. The heating rate is plotted against the inverse of that temperature to find the activation energy. In the "thermal jump" method, the temperature is "jumped" from T1 to T2 at a specified conversion; thus rates can be measured at two temperatures at the same degree of conversion and the activation energy can be directly estimated with the aid of the Arrhenius equation (3). Each of these methods has its own set of advantages and disadvantages. In principle, the "jump" method is ideal to determine activation energies. However, it is difficult to use at low temperatures where the reaction rates are low and the signal-to-noise ratio is low.

Scanning Auger Spectroscopy: Auger electron spectroscopy is an analytical technique to determine the elemental composition of the top few atomic layers of a sample's surface. A Physical Electronics Model 545 scanning Auger microprobe housed at the Physics department at the University of Missouri-Rolla has been used for all experiments.

Every element produces a unique Auger spectrum. The entire analysis is conducted in a high vacuum chamber.

An additional feature of the Auger analysis chamber is the ability to carefully abrade the surface by argon ion bombardment. This sputtering method removes surface material. A sputter profile involves monitoring the Auger electron signal from a few selected elements as the sample is sputtered away by the argon ion beam, producing an elemental composition profile as a function of depth. The sputtering rate used in our experiments varied from 19 to 50 nm (190 to 500Å) per minute. The sputtering can be stopped at any time during the profiling and a survey scan or element map acquired, the profiling then is resumed. Mapping in this fashion gives three-dimensional information about the sample composition.

Gas Chromatography – Mass Spectrometry (GC-MS): Gas chromatography is an analytical method used to separated components of a complex mixture. A Varian 3600 CS gas chromatograph with a Saturn GC/MS/MS detector has been used to identify volatile ETFE degradation products. The polymer is degraded directly in a Varian Chromatoprobe pyrolyzer attached to the GC/MS. Preliminary separation is accomplished by a short (3 m) section of blank column used as a flow restrictor.

Fluid Sorption: Films approximately 60 x 6 mm were immersed in the fluid of interest contained in 2.5 x 15 cm culture tubes which were placed in a thermostatted aluminum block. At appropriate intervals, the samples were removed from the culture tubes, blotted dry, placed in a tared weighing jar, weighed on a digital electric balance and returned to the oven in less than 15 seconds. Fluid desorption was accomplished by placing the sample on a watch glass in an oven at the temperature of interest.

Infrared Spectroscopy. IR spectroscopy was used to examine the solid polymers to ascertain what products were formed and what compounds were lost as a function of both radiation and thermal degradation. Fourier transform attenuated total reflectance infrared (FT-ATR-IR) was used to conduct the experiments. The instrument was located at the Monsanto Co. Research laboratory in Creve Coeur Missouri. The polymer was placed on a polished silver stage under a microscope with both optical and ATR capabilities. Normally, 128 scans were used to form a spectra. ETFE samples degraded in both the presence and absence of conductor in air for time intervals ranging from 20 to 60 hours at temperatures between 240° and 290°C were analyzed by FT-ATR.

Crystallinity/morphology: The crystallinity was evaluated by differential scanning colorimetry (DSC) in a nitrogen atmosphere at a scan rate of 10°C/min in a Thermal Analysis DSC (TA 2910 Modulated DSC).

4.0 Results and Discussion

An in-depth investigation of the thermal degradation of a typical commercial polymer, such as ETFE, has all of the complexities associated with industrial polymers. It is a semi-crystalline copolymer prepared from a stoichromatric ratio of ethylene and tetrafluoroethylene, it contains an anti-oxidant, and a flame retardant and it is irradiated with high-energy electrons in the presence of a "promoter" to enhance its high temperature mechanical properties. Furthermore, in actual use this material is in direct contact with an active metal surface whose chemistry changes with time. This study used a combination of physical analytical methods to determine the degradation mechanism of this complex material in an environment which simulated its actual use. If the degradation process can be accurately measured and modeled, the durability or lifetime of the polymer in contact with the active metal can be estimated.

The primary mode of failure of thermoplastic electrical insulation arises from a loss in mechanical properties, leading to cracking. The primary cause of cracking is embrittlement of the insulation due to thermo-oxidative degradation. The research was concerned with three aspects of the overall degradation process:

- degradation kinetics of ETFE polymer
- degradation of ETFE in the presence of metal catalyst, and
- physical and chemical changes in the composition of the conductor.

Degradation of ETFE: The degradation of ETFE was studied by four different methods:

1. isothermally: in an air circulating oven at temperatures between 150°C and 300°C

2. isothermally is the TGA system (air, oxygen, or nitrogen atmosphere) at temperatures between 220°C and 320°C

3. dynamically in the TGA system (air, oxygen, or nitrogen atmosphere) at heating rates between 0.5 and 20°C/min, and

4. in the TGA using the kinetic-jump method to oscillate between temperatures, usually between 300°C and 310°C.

These methods compliment each other and provided answers to different portions of the ETFE degradation puzzle. Typical results from each of these methods are discussed below.

Isothermal Thermo-Oxidative Degradation: A typical fractional weight loss curve for the degradation of ETFE insulation at 280°C in an air circulating oven is shown in Figure 1. The radiation dose varied from 0 to 48 Mrads. Isothermal ETFE weight loss curves indicate a complex, multistep degradation process. Within the first hour, ETFE loses about 1% of its original weight due to volatilization of low molecular weight compounds.

During the second stage of the degradation process, higher molecular weight compounds, primarily additives such as anti-oxidants and cross-linking agents, are lost at a rate which decreases exponentially with time. The products were analyzed by GC/MS and the resulting polymer was investigated by FTIR. After the initial weight loss of the low molecular weight compounds, the weight loss is linear with time, suggesting a zero-order degradation process. This latter step is strongly dependent on temperature and radiation dose. The preliminary model described previously (4) was expanded into a four-parameter phenomenological model to describe the degradation process:

$$\alpha = A \cdot t - B \cdot \exp(-C \cdot t) + D \cdot H(t \equiv 0) \qquad (1)$$

where

α = degree of conversion

A = linear degradation coefficient

B = additives coefficient

C = exponential rate coefficient

D = Coefficient for volatilization of low molecular weight compounds

H = step function occurring at t $\cong$ 0

The A parameter reflects weight loss of the ETFE polymer, B indicates the amount of additives in the insulation, C reflects the rate at which additives are lost, and D reflects the compounds which evolve during heating. The effect of both temperature and radiation on these variables was determined. The best fit to the experimental data yielded the following expressions:

$$A = 1.13\times10^{10}\exp\left(-157(kJ/mol)/RT\right) + 2.69\times10^{4}\cdot X\cdot\exp\left(-114(kJ/mol)/RT\right) \quad (2)$$

$$B = 2.49\times10^{3} + 4.14\times10^{-4}X \quad (3a)$$

$$D = 5.49\times10^{-3} + 2.35\times10^{-4}X \quad (3b)$$

where

X = radiation dose (MRad), R = gas constant, and T = temperature (K), respectively. *C is essentially independent of dose.*

ETFE wire (insulation and unmodified conductor) samples with radiation doses from 0 to 48 MRads were degraded in an air circulating oven at temperatures ranging from 240°C to 300°C. Typical degradation curves, in which the amount of polymer remaining., [(1-α) where α is the degree of conversion] as a function of time at 260°C are shown in Figure 2. It is readily apparent that the higher the radiation dose, the more rapidly the polymer degrades. For example the time for the sample to incur a 10% weight loss in the presence of metal is only one-third that required in the absence of metal; this comparison is summarized in Table 2. Weight loss in the presence of the metal is not a linear function of time, but shows a dependence on the degree of conversion, α. Weight loss curves exhibit a strong dependence on dose for irradiation less than 10 MRads but for the heavily irradiated samples, i.e. 29, 38 and 48 MRads, the rates of weight loss are essentially the same.

Isothermal Thermogravimetric Analysis: Isothermal TGA was used to (1) investigate short-term degradation, and (2) determine the effect of different environmental gases. This data serves as an excellent check on isothermal oven experiments.

The effect of temperature on the isothermal degradation process is illustrated in Figure 3 where the weight loss is shown as a function of time at temperatures ranging from 240°C to 300°C for insulation irradiated at 48 MRads. The data is consistent with that observed in the isothermal oven studies.

Non-Isothermal TGA: Two non-isothermal TGA methods were used to estimate the kinetic parameters for the ETFE degradation process, as a compliment to isothermal methods described above. The respective merits of the Flynn and Wall (2) method and the kinetic jump method (3) will be discussed, along with a comparison of results.

Kinetic Jump: The kinetic jump method is a technique to obtain the activation energy for a degradation process in a selected temperature interval at a given degree of conversion (3). During a given run the isothermal temperature is cycled between two or more temperatures and the activation energy (ΔE) calculated by measuring the rates at two temperatures and using the simple form of the Arrhenius equation:

$$\Delta E = R \cdot T_1 \cdot T_2 / \left\{ \Delta T \cdot \ln\left[R(T_2)/R(T_1) \right] \right\} \qquad (4)$$

where $R(T_2)$ and $R(T_1)$ are the rates of the temperatures T_2 and T_1, respectively. The jumps can be conducted at a series of temperatures, degrees of conversion, and radiation doses, and all other kinetic parameters, such as reaction order, are eliminated. The practical limits of this method are restricted by the low signal-to-noise ratio at low temperature when degradation rates are small.

Dynamic TGA: In dynamic TGA samples are heated at different heating rates generating a series of curves of weight loss versus temperature. The rates of degradation at the different heating rates can be analyzed. The data can be analyzed according to the Flynn and Wall method which is derived from the non-isothermal kinetic equation

$$d\alpha/dt = f(\alpha) * k(T) * g(\alpha, T) \qquad (5)$$

where

α = degree of conversion

T = temperature

This method assumes that the degree of conversion and temperature variables are separable, therefore $g(\alpha,T)=1$. As in the thermal jump method, k is assumed to have an Arrhenius dependence, leading to the equation

$$d\alpha/dt = f(\alpha) * A * \exp(-E_a/RT). \quad (6)$$

The mathematics and approximations involved in this method have been described by several authors, for example see Ref 1. Multiple experiments at different heating rates are compared at the same degree of conversion, eliminating the effect of the conversion term, and the activation energy can be obtained directly from the TGA data.

Experiments were conducted in air, oxygen, and nitrogen on ETFE samples heated at 1, 2, 5, 10, 15, and 20°C/min. Activation energies were found at 0.5% conversion intervals between 5% and 9.5%, the results are summarized in Table 3. Activation energies from irradiated samples degraded in air averaged 155 kJ/mol. Unirradiated samples behave differently than irradiated samples and exhibit a much higher activation energy, in the range of 235 kJ/mol. Large deviations (about 10%) were noted in the samples irradiated to 29 MRad and 38MRad. At the high degrees of conversion, the activation energies decreased, with an average decrease of 6% through the conversion range. Samples degraded in nitrogen were more stable, with temperature factors above 200 kJ/mol at all irradiation doses. Samples degraded in oxygen are different! A series of experiments similar to those described above on the insulation, for wire samples are summarized in Table 4. The error associated with these experiments is greater than that associated with insulation alone because the rates are a stronger function of the degree of degradation.

The temperature factor for unirradiated ETFE is approximately 100 kJ/mol lower than for the sample irradiated at 6MRads. For radiation doses greater than 6MRads the activation energies in oxygen are between 150 and 170 kJ/mol. The degradation of wire in oxygen is more complex. At least two different degradation processes were observed; their relative magnitudes depend upon the TGA heating rate. A deconvoluted degradation rate curve is shown in Figure 4. Surprisingly, the temperature coefficients determined by a simple Arrhenius plot suggest that the higher temperature reaction has a lower temperature coefficient. Experiments in air and oxygen reach 5-10% conversion at lower temperatures than in nitrogen, which further complicates a direct comparison between kinetic parameters.

Isothermal TGA

Isothermal TGA experiments are used to explore the degradation process at low temperatures. These results can be directly compared with isothermal TGA experiments at higher temperatures by appropriate kinetic expressions, however, it should be noted that in the oven experiments the reaction atmosphere is restricted to air.

The insulation exhibits a constant weight loss rate throughout the conversion range of interest (3% - 30%). The weight loss rate is linearly dependent on irradiation dose, and an Arrhenius temperature coefficient of 150 kJ/mol was observed in the range of 240° to 280°C. Experiments in nitrogen shows the same general trends, with a lower degradation rate. At high temperatures (320°C and above in air, or 300°C and above in oxygen), the rate of weight loss is not linear with time, see Figure 5. At low conversions, the degradation rate passes through a minimum which rapidly increases for conversion of

the order of 15-20%. At high conversions, the degradation rate decreases slowly. This phenomenon is much more pronounced in wire, i.e. in the presence of the conductor.

Isothermal Jump Method TGA. The isothermal jump method offers an alternative method to dynamic TGA for determining temperature dependence of the degradation process. A single sample is degraded at two alternating temperatures (typically 300°C and 310°C), while the resulting weight loss rate is measured by the TGA. At specified conversions, the temperature "jumps" from one temperature to the other. Over this small of a temperature range, it is assumed that the experiment yields weight loss rates at two different temperatures for the same conversion. Using the ratio of these two degradation rates, an Arrhenius temperature dependence yields a temperature factor. This method is more time-consuming than dynamic methods, and more vulnerable to errors from noise, but lacks the systematic error from sample variation. For ETFE measurements in air, the activation energies were comparable to dynamic data, with more scattering, due to experimental error. A notable difference occurred in unirradiated ETFE insulation where the activation energies were 130 kJ/mol (compared to 200 kJ/mol in dynamic experiments). In nitrogen, the temperature factors were lower than observed in the dynamic method, between 150 and 170 kJ/mol. In oxygen, the data were consistent i.e. the temperature factors were essentially the same for both methods.

The degradation of ETFE in the presence of conductor is different than in its absence. In air the temperature factors are between 120 and 135 kJ/mol and exhibit less scatter than observed in polymer, this probably arises from the higher degradation rates thereby increasing the signal-to-noise ratio. Degradation of irradiated wire samples in nitrogen also showed lower temperature factors (130-150 kJ/mol), however with greater

experimental scatter. Some of the differences in the results obtained by dynamic and isothermal jump experiments may result from the different temperature regions used in the two experiments.

Infrared Analysis: When aged as polymer, the samples were flattened directly for IR analysis, while the insulation from wire samples was separated from the conductor by cutting the polymer lengthwise down the wires, and the two pieces were flattened and analyzed. Both sides of the sample could be analyzed by this method; the surface in direct contact with metal surface and the surface exposed to the ambient environment. A typical FT-ATR difference spectra, in which the spectra from a sample aged for 53 hours at 270°C (irradiated to 6MRad prior to aging) minus the spectra from an unaged sample) is shown in Figure 6. The IR spectrum shows two distinct regions: 1) the range 1750-1500 cm^{-1} is attributed to polymer oxidation, i.e. carbonyl, and 2) the range 1000-1350 cm^{-1} is primarily due to C-F bonding. The broad peak (1750-1500 cm^{-1}) increases with aging and is more pronounced in samples in which ETFE is in contact with the Ag/Cu conductor. The IR spectral data is summarized in Table 5.

Aging of the Silver/Copper Interface: The major objective of this project is to determine the overall durability of the polymer/metal system, i.e. the insulation and the conductor. Although usually neglected, the conductor is a complex system which changes with time. In many electrical systems, the conductor is a copper wire coated with a thin layer of metal, such as silver, primarily to enhance solderability. However, during prolonged use at high temperature, copper can diffuse through the silver layer, markedly changing the characteristics of the metal. Active metals, such as copper, silver or their oxides are well known for their catalytic activity. We have observed in some instances

that the metallic diffusion process is a function of the polymer coating. Therefore, the degradation of the polymeric system changes with time. We have examined this phenomenon by the use of scanning Auger spectroscopy.

Of particular interest is the diffusion of copper through the silver layer and the subsequent oxidation of the copper layer. [A layer of silver, $5x10^{-5}$ cm thick, is applied over metallic copper.] The concentration of Ag, Cu, C, O, Sb, and Cl were monitored following controlled thermal aging as a function of depth by scanning Auger spectroscopy; a typical depth profile is shown in Figure 7. The interface between the silver and copper layers of the unaged samples is relatively sharp, approximately $5x10^{-5}$ cm thick, and contains only silver and copper. At typical scanning Auger trace of an aged sample is illustrated in Figure 8. In this particular trace, the sample had been irradiated to a total dose of 48 MRads and aged in an air environment for 181 hours at 250° C. It is important to note that the surface is essentially a layer of copper oxide (the approximate stoichiometry is $Cu_{2.7}O$ based on atomic ratios) $6x10^{-5}$ cm thick. A small amount of Sb was also observed on the surface: the source of Sb may be from SbF_5 which is often added to insulation as a flame retardant. The diffusion of copper and its subsequent oxidation was investigated as a function of 1) radiation dose, 2) aging temperature, and 3) presence or absence of polymer coating on the diffusion process. The effect of radiation dose, temperature, time of aging, and presence or absence of polymer on the diffusion process is illustrated in Figure 9. The diffusion of copper through the silver layer is readily apparent.

The effect of the polymer on the metal surface during aging has a large influence on the diffusion/oxidation process. Most samples aged as conductor (in absence of

insulation) displayed a copper and oxygen layer on their surface, with little or no silver present. The composition of this layer (atomic ratio of copper to oxygen) shifted from 1.5:1 on the sample surface to 2:1 at depth greater than 500 nm. These ratios suggest that the surface layer consists of CuO while the interior region is a mixture of CuO and Cu_2O. The thickness of the copper oxide layer increases as aging temperature and time increase, and is typically between 300 and 600 nm thick. A silver layer follows the copper oxide layer, and the bulk interior is copper only. As expected, the oxygen concentration decreases with depth; for example see Figure 8. When the conductor is covered with ETFE, the diffusion is more rapid and the copper surface layer is thicker; the ratio of copper to oxygen at the surface is approximately 3:1 and decreases as one moves into the bulk sample, see Figure 9. The silver profile is broad suggesting that the silver is not stationary but also diffuses. However, the rate of diffusion of silver in copper is significantly slower than the diffusion of copper through silver.

Analysis of Degradation Products. The primary products identified by GC/MS analysis of the effluent products were HF and fluorinated hydrocarbons of the parent compound. The primary mass spectral peak was at $m/z = 147$ and corresponds to $[CH_2CH_2CF_2CF_2]^+$. Ions corresponding to higher oligimers of the parent molecule were also observed.

Microscopy: Optical microscopy was used to observe changes in both the surfaces of the insulation and conductor both before and after degradation/aging. The samples were normally viewed at a magnification of 900X. The same samples were also studied by ATR-FTIR. In many instances the silver layer was observed to "peel" off the copper conductor. For example, the insulation removed from aged wire (i.e. sample aged for 20

ours at 270°C) displayed long thin metallic stripes at a 45° angle to the axial direction of the sample (the length of the wire). The silver color and width of these stripes, combined with the match to the helical packing of the wire strands, suggest that the silver layer on the conductor adheres to the polymer surface. As the irradiation dose, temperature, or degradation time increases, the adhesion to the polymer becomes more pronounced. The conductor displayed corresponding color changes, with a silver color appearing at the sides of a strand, and shades of red or orange (indicative of copper compounds) in the center of individual strands. This latter phenomenon indicates that the diffusion/oxidation process is strongly influenced by the presence of the polymer coating.

The SEM analysis showed, that in many cases, the silver layer was strongly attached to the polymer layer and upon removal of the insulation from the wire, the silver adhered to the polymer. This phenomenon is illustrated in Figure 10 where the center region of the photo shows a layer of silver and bare copper on both the left and right sides. This particular sample was irradiated to a dose of 9 MRad and aged as wire for 20 h at 270°C. The interior surface of the insulation had a smooth surface, while the surface layer contained many bumps and crevasses. In another location on the same sample the outer layer peeled away and an elemental analysis (EDS) of the interior peeled region indicated that the adhering surface was 83% silver and 17% copper. The composition of the layer and its location suggest that this is the silver coating, and that it debonds from the copper and attaches to the polymer during aging. This observation agrees with the optical microscopy experiments.

SORPTION OF FLUIDS

The sorption of CS_2 into amorphous PPS as a function of temperature is illustrated in Figure 11. The sorption process actually consists of four separate regions: 1) an initial region in which 1 – 3 wt% is rapidly sorbed, 2) a region which is eventually linear with root time (pseudo-Fickian region), 3) a maximum value, and 4) a "pseudo-equilibrium" region in which the solubility is essentially constant. The sorption of toluene in amorphous and crystalline PPS at 24° is shown in Figure 12. The sorption process is similar to that observed with CS_2 except that the sorption in crystalline PPS is significantly less.

The initial rapid sorption probably arises from stress enhance sorption due to surface stresses. The active depth of the stressed region can be estimated: if the "surface" is saturated, it comprises 10% of the sample thickness (2 wt% divided by the equilibrium solubility, 20 wt%). The films are 0.262 mm thick and contain two active surfaces, thus, the stressed surface is approximately 0.013 mm (or 13 μm) thick.

The second region corresponds to the normal sorption of an organic fluid in a polymer. The shape of the curve is governed by the rate of penetration of the fluid compared to the rate of relaxation of the swollen polymer behind the advancing front. The pseudo-Fiebian region, corresponding to weight gain which is a linear function of the square-root time, indicates that the rate of diffusion is greater than the rate of relaxation. The maximum is the sorption curve and the associated gentle decrease in amount sorbed arises because the polymer undergoes solvent induced crystallization. Small amounts of solvent are trapped in or adjacent to the crystals, the solvent is slowly "squeezed" out of the crystals as the sample slowly approaches equilibrium. This is in sharp contrast to the

sorption of fluids, such as water, in epoxies where the sample continues to sorb water, even after thousands of hours, as the resin slowly relaxes.

The sorption of CS_2 and toluene into crystalline PPS exhibit quite different phenomena. CS_2 is readily sorbed in crystalline PPS although its rate of sorption is approximately one-hundredth that of the sorption rate observed in amorphous PPS. However, its equilibrium solubility in crystalline PPS is only 15% less than that observed in amorphous PPS; a typical sorption curve is shown in Figure 13. Both solubility and rate of diffusion of toluene into crystalline PPS are small: see Figure 12.

Of particular interest to the overall mechanism is the resorption of a fluid into a resin from which the initial saturating penetrant has been removed. This particular study actually consisted of 4 separate experiments: resorption of either CS_2 or toluene into a resin originally saturated with CS_2 or one that had been saturated with toluene: this can be abbreviated as CS_2/ CS_2, CS_2/toluene, toluene/ CS_2 or toluene/toluene. These results are summarized in Figures 14 and 15, respectively. The sorption and subsequent resorption of CS_2 from initially amorphous PPS at 26°, 33°, and 40°C are shown in Figure 16. Following the first sorption the samples were completely absorbed at 65°C in a vacuum oven. The solubility is essentially independent of temperature, approximately 17 wt%, compared to the initial solubility of approximately 20 wt%.

It is important to note the vast difference in the sorption of CS_2 and toluene, particularly with respect to resorption. Although CS_2 and toluene have significantly different vapor pressures at any given temperature, i.e. the boiling points of CS_2 and toluene are 40° and 110°C, respectively, the primary difference with regard to sorption is their molecular size. At room temperature, the molar volumes of CS_2 and toluene are

58.7 and 106 cm^3, respectively. The average molecular volume of CS_2 and toluene were calculated and reported to be 49 and 92 $Å^3$, respectively (5).

Amorphous PPS can be thermally crystallized by heating it above the glass transition temperature. Typical DSC thermograms for PPS heated above and below its T_g(85-90°C) are shown in Figure 17. Three noticeable features are exhibited in the thermogram of a typical amorphous PPS sample (shown in figure 17A): α is the T_g at about 85-90°C, β is the "cold crystallization: exotherm at about 130°C and γ is the melting endotherm at about 290°C. The magnitude of the "cold crystallization" peak decreases when PPS is heated at temperatures above 70°CC and is absent when PPS is heated at temperatures at 110°C and above. According to Brady (6), the heat of crystallization of 100% crystalline PPS is 80kJ/kg. The ratio of the exotherm (at 130°C) or endotherm (at 290°C) to the heat of the crystallinity gives the degree of crystallinity produced during the "cold crystallization" or the degree of crystallinity in the sample at the time of melting. (i.e., $f_C = H_M/H_C$), respectively. The "cold crystallization" exotherms are shown in column 2 of Table 6 and the crystallinities produced during "cold crystallization" are shown in column 3 of Table 6. The % "cold crystallinity" in a typical amorphous PPS sample gives the maximum % "cold crystallinity: which, according to Table 6, is about 28%. The melting endotherms and their associated crystallinities are shown in columns 4 and 5 of Table 6, respectively. The average of all the melting endotherms, H_M, is 32.1 J/g which corresponds to a crystallinity of about 40%. Column 6 of Table 6 displays the degree of crystallinity of the samples after being dried for 24 hours but before being scanned. If the sample is already partially crystallized, the maximum "cold crystallinity" it can achieve is 28% therefore the amount of crystallinity

produced during drying is equal to the maximum % "cold crystallinity" (28%) minus the % "cold crystallinity" observed in the thermogram. The absence of the "cold crystallization" peaks in Figure 17 D and E (dried at 110°C and 130°C respectively) suggest that the degree of crystallinity thermally induced is greater than or equal to 28%. The PPS thermograms resemble the thermograms of PEEK (7) where the crystallization exotherm is much smaller than the melting endotherm. This observation has been explained by noting that the crystallization process in PEEK continues (after the initial cold crystallization) during the DSC scan to form "more perfect crystals" which melt at about 345°C (7).

Typical weight gain curves in which % weight gain is plotted as a function of square-root time (Fickian form) for different drying conditions are summarized in Figure 18. An expanded view of this graph showing the first 25 hours is shown in Figure 19. A typical weight gain curve for an amorphous sample (as received) is shown in Figure 20.

In general, sorption curves for samples dried at or below 100°C show three major regions (see Figure 20): (A) a rapid initial period which exhibits an accelerated absorption, (B) a steady weight gain which is approximately linear with square root time, and (C) the weight gain curve rising to its maximum value of about 11.5%. This latter phenomena may be due to an expulsion of a small amount of fluid from the crystalline regions while the system attains equilibrium, or may arise from the extraction of a small amount of low molecular compounds into the immersion fluid.

The initial sorption for samples dried at or below 100°C (see Figure 19) occurs approximately within the first 10s. This sorption however, is not seen for samples dried at or above 110°C suggesting that initial sorption is associated with surface morphology.

The crystallinity of samples dried at or above 110°C is at least 28% whereas the crystallinity of samples dried at or below 100°C is below 28%. All the curves show a linear relationship with square root time after the initial rapid sorption suggesting that Fick's laws are applicable and pseudo-Fickian-like diffusion coefficients can be estimated. A marked decrease in the rate of diffusion (which is proportional to the square of the slope) for samples dried at 110°C compared to that for samples dried at or below 100°C, suggest that diffusion is a function of drying conditions. The ratio of the slope for samples dried at 110°C to that for samples dried at or below 100°C is approximately one-sixteenth implying that the diffusion coefficients for samples dried at 110°C is approximately 250 times smaller than that for samples dried at or below 100°C since diffusion is proportional to the square of the rate of diffusion.

Table 1
Properties of Electrical Wire System

Sample	Radiation Dose (MRad)	Melting Point* (°C)
A	0	265.3
B	6	261.5
C	9	259.1
D	19	255.2
E	29	251.6
F	38	249.1
G	48	246.7

*Measured by DSC: the minimum is the melting endotherm

Table 2. Comparison of time (hours) to 10% ETFE weight loss from polymer alone and in contest with Ag/Cu at 260°C

Dose (MRads)	6	9	19	29	38	48
Insulation (min)	17700	13900	9000	6900	4500	4050
Wire (min)	2900	2800	1800	1700	1475	1400

Table 3

Activation energies (kJ/mol) from the dynamic method for the degradation of irradiated ETFE as a function of dose, atmosphere and degree of conversion

Environ-	Radiation	Degree of conversion (%)							
ment	(Mrads)	5	6	7	8	9	10	ave	σ*
Air	0	241	238	236	235	233	232	236	3.3
Air	6	152	156	157	158	157	157	156	2.1
Air	9	164	162	160	158	158	157	160	2.7
Air	19	162	160	158	157	156	155	158	2.6
Air	29	185	182	178	173	170	166	176	7.3
Air	38	145	143	143	142	141	141	143	1.5
Air	48	169	161	156	154	152	150	157	7.0
Nitrogen	0	221	223	225	228	231	234	227	4.9
Nitrogen	6	200	202	202	205	206	209	204	3.3
Nitrogen	9	204	206	212	219	225	229	216	10.2
Nitrogen	19	219	222	230	240	247	250	235	13.0
Nitrogen	29	176	179	184	190	197	203	188	10.5
Nitrogen	38	210	212	226	249	259	269	238	25.0
Nitrogen	48	237	240	246	254	260	261	250	10.2
Oxygen	0	146	147	148	149	150	150	148	1.6
Oxygen	6	101	101	103	106	105	110	104	3.4
Oxygen	9	169	170	170	169	168	167	169	1.2
Oxygen	19	181	184	186	187	186	184	185	2.2
Oxygen	29	198	195	194	193	193	192	194	2.1
Oxygen	38	200	202	203	203	203	204	203	1.4
Oxygen	48	225	218	214	212	209	206	214	6.8

σ* Standard deviation, 1σ

Table 4

Activation energies (kJ/mol) from the dynamic method for the degradation of irradiated ETFE in the presence of conductor as a function of dose, atmosphere and degree of conversion

Environ-ment	Radiation (Mrads)	Degree of conversion (%)								
		4	5	6	7	8	9	10	avg	σ*
Air	0	197	197	197	198	197	196	196	197	0.7
Air	6	162	158	155	154	153	153	152	155	3.5
Air	9	174	169	165	161	158	155	153	162	7.6
Air	19	163	158	157	154	153	152	151	155	4.2
Air	29	165	158	157	155	153	152	151	156	4.8
Air	38	157	156	154	151	150	148	147	152	3.9
Air	48	168	161	157	154	152	150	148	156	6.9
Nitrogen	0		241	242	241	240	239	239	240	1.2
Nitrogen	6		202	202	201	202	208	212	205	4.5
Nitrogen	9	208		213		226		239	222	13.9
Nitrogen	19	209		214		230		243	224	15.5
Nitrogen	29	202		207		217		221	212	8.8
Nitrogen	38	211		218		225		225	220	6.7
Nitrogen	48	212		214		224		226	219	7.0
Oxygen	0		129	130	131	133	133	134	132	2.0
Oxygen	6		121	121	123	124	125	125	123	1.8
Oxygen	9		149	147	148	148	148	146	148	1.0
Oxygen	19		163	165	164	163	160	159	162	2.3
Oxygen	29		166	165	164	163	160	159	163	2.8
Oxygen	38		166	166	164	164	161	159	163	2.8
Oxygen	48		173	170	169	166	164	162	167	4.1

σ: Standard deviation, 1σ

Table 5
Summary of FT-IR Spectra

Unaged ETFE Spectrum peaks	Source
2980(m), 2960 (w), 2890 (w)	C-H stretching
1475(w), 1451(s)	CH_2 scissoring
1320-1330(s)	CH_2 twisting
1252 (vs)	CF_2 asymmetric
1170 (vs)	C-C skeletal
1115 (vs)	CF_2 symmetric
1050 (vs)	CF_2
972(m)	
665(s),510(s)	CF2
Additives and crosslinks	
1700	Carbonyl stretch from TAIC
1170	Tertiary C-H (from crosslinks)
1120-1010	Tertiary C-F

Observed both in literature spectra and in description of Pirozhnaya and Tarutina. *J. Appl. Spectroscopy* **34** 539-541 (1981).
Experimental unaged ETFE spectra had weaker C-H stretching bands

Time substracted spectra peaks	Explanation
4000 – 3600 (m, broad)	OH
2980, 2960, 2890 (m)	CH stretch, seen in 290C, 21 hr samples
1700 – 1500 (m, broad)	Carbonyls (an overlay of several in 270C, 53 hour samples
1742 (m)	Dialkyl ketone (seen in 290C, 21 hr samples) or $-C=DF_2$
1617 (m)	C = C
1451 (m)	CH_2
1322	CH_2
1165	Tertiary CH
1038 (vs)	Possible shift of CF_2 peak due to changes in substituents
1322, 1165 peaks may be dependent on subtraction parameters	

Table 6: DSC Analysis of PPS

Reference Value: 80 kJ/kg

Temperature (C)	"Cold" Crystallization Exotherm (J/g)	% "Cold" Crystallization	Melting endotherm (J/g)	%Final crystallinity	% Initial crystallinity*
As received	22.3	27.88	32.90	41.13	0.0
70	22.4	28.00	32.57	40.71	0.0
100	8.2	10.27	31.87	39.84	17.7
110	~0	~0	32.04	40.05	>28
130	~0	~0	31.11	38.89	>28

*Initial Cyrstallinity = MAX(% "Cold Crystallinity") - % "Cold Crystallinity" measured

References

1. Clarence J. Wolf and R.S. Soloman, "Environmental Degradation of Aromatic Polyimide-insulated Electrical Wire," *IEEE Trans. Elec. Insulation* 19, 265 (1984).

2. J.H. Flynn and L.A. Wall, "Thermal Analysis of Polymer by Thermogravemetric Analysis," *J. Res. Natl. Bur. Stand.*, Ser. A 70 (6) 487-523 (1966).

3. J.H. Flynne "Aspects of Degradation and Stabilization of Polymers," Chap. 12 pp. 573-603, H.H.G. Jellinck, ed. Elsevier, Amsterdam, 1978.

4. C.J. Wolf, S.C. Hager, and N.P. Depke, "Thermo-Oxidative Degradation of Irradiated Ethylene Tetrafluorethylenes," in *Oxidative Behavior of Materials in Thermal Analytical Techniques*," Eds. A.T. Riga and G.H. Patterson STP 1326 ASTM, 1997 pp. 116-127.

5. Clarence J. Wolf, J.A. Bornmann, and M.L. Gurpon, "The Absorption of Organic Liquids in Poly (Aryl-Ether-Ether-Ketone) [PEEK]" *J. Polm. Sci.* 13: Polym Phys. 29 1533-1539 (1991).

6. D.J. Brady, *J. Applied Polym. Sci., Phys. Ed.*, 20, 2541 (1976).

7. C.J. Wolf and J.A. Bornmann, "Differential Scanning Coloremetry (DSC) to Determine Crystallinity in PEEK," *Soc. Adv. Mater. Proc. Eng.*, 34, 1167 (1990).

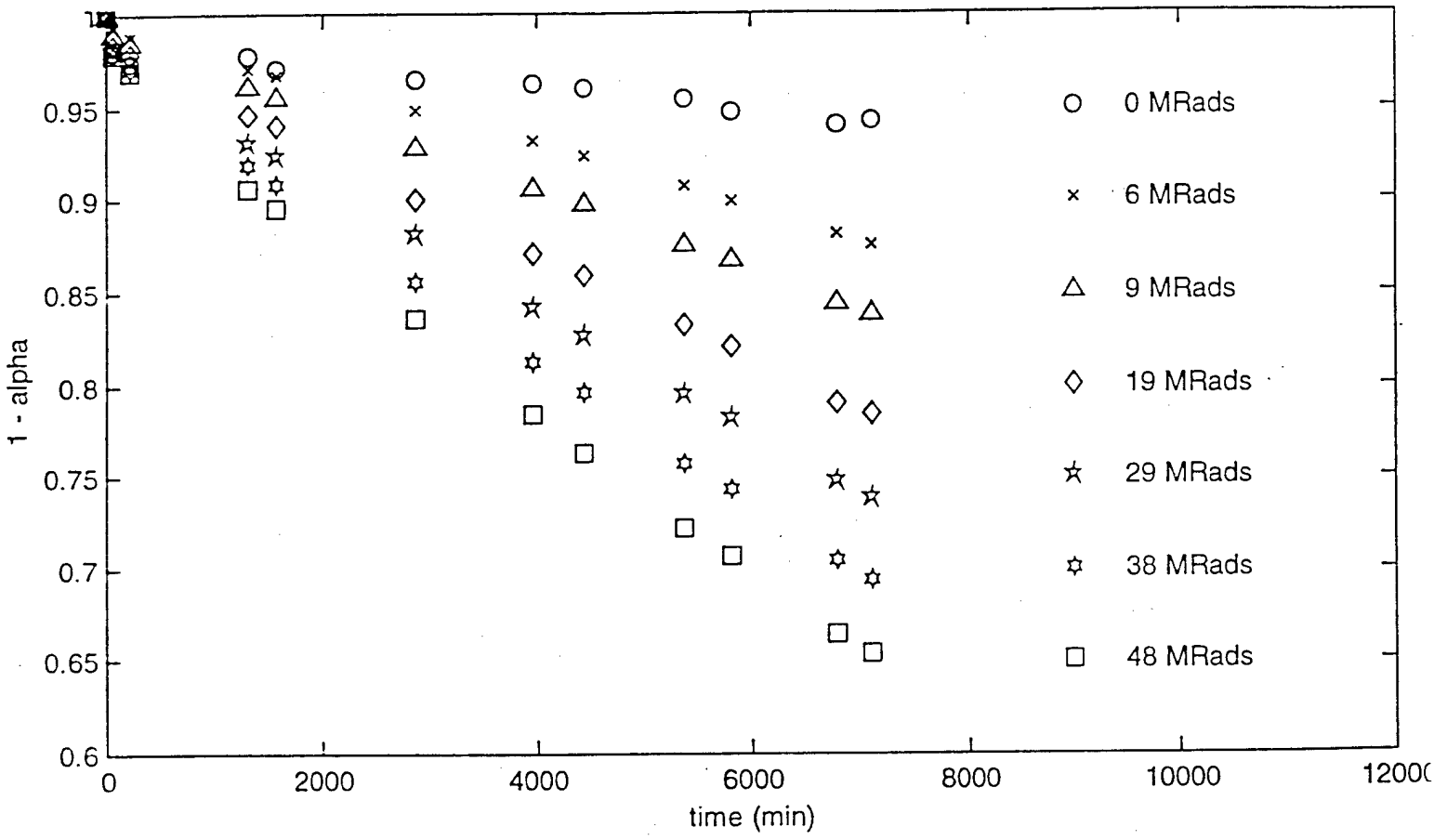

FIGURE 1. Fractional weight loss (1-α) remaining as a function of time for the thermal degradation of irradiated ETFE.

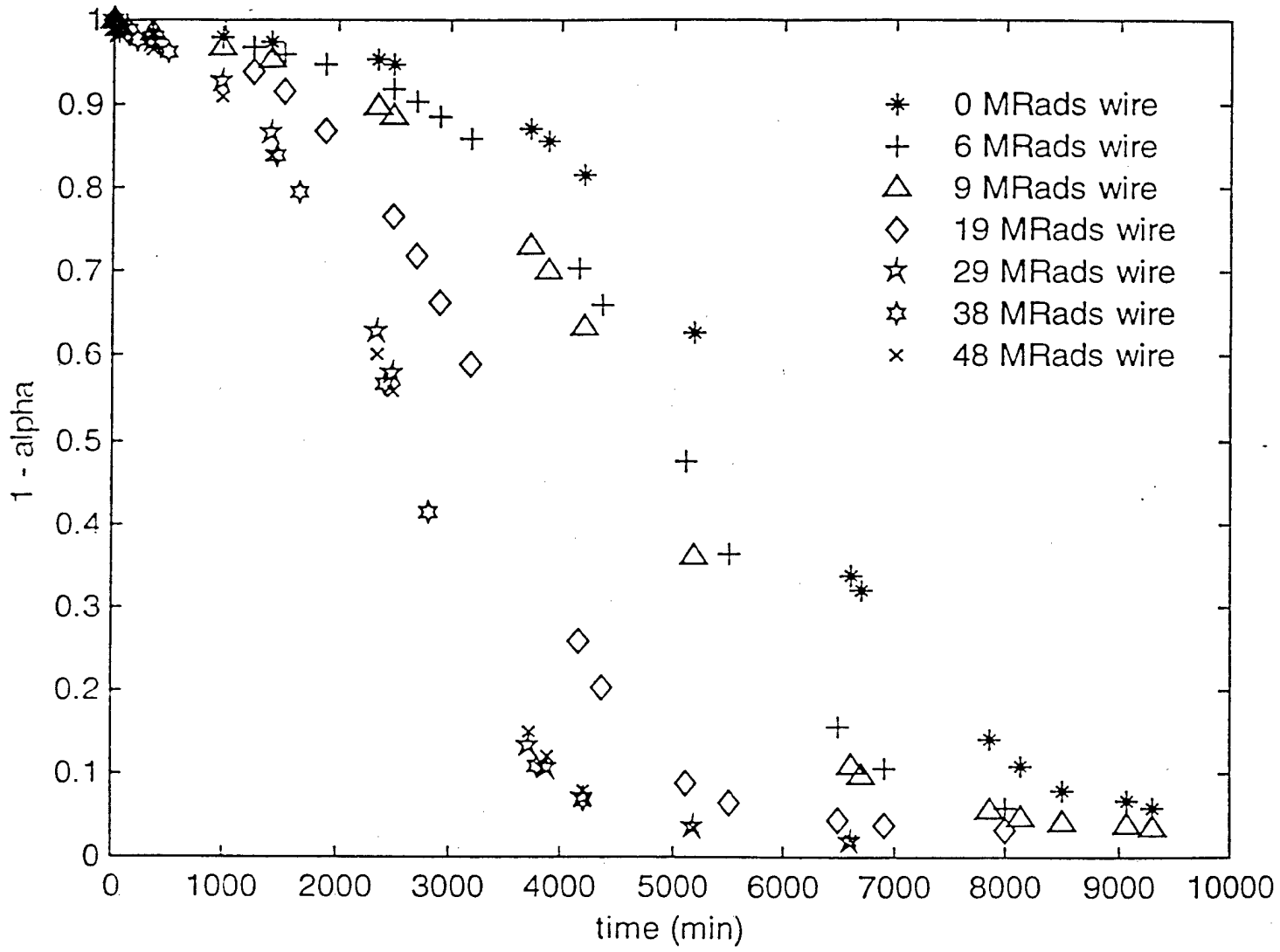

FIGURE 2. Percent weight loss for the thermal-oxidative degradation (260°C) of wire as a function of time and radiation dose.

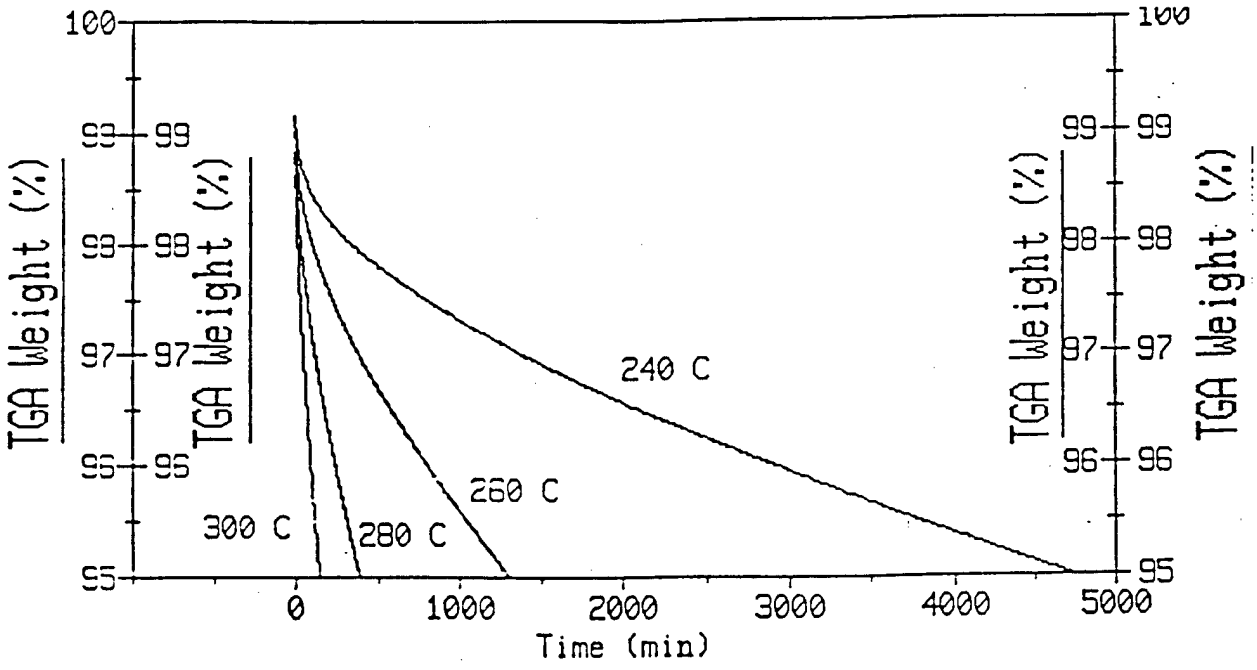

FIGURE 3. Weight loss as a function of time for the isothermal degradation of ETFE irradiated to a total dose of 48 MRads.

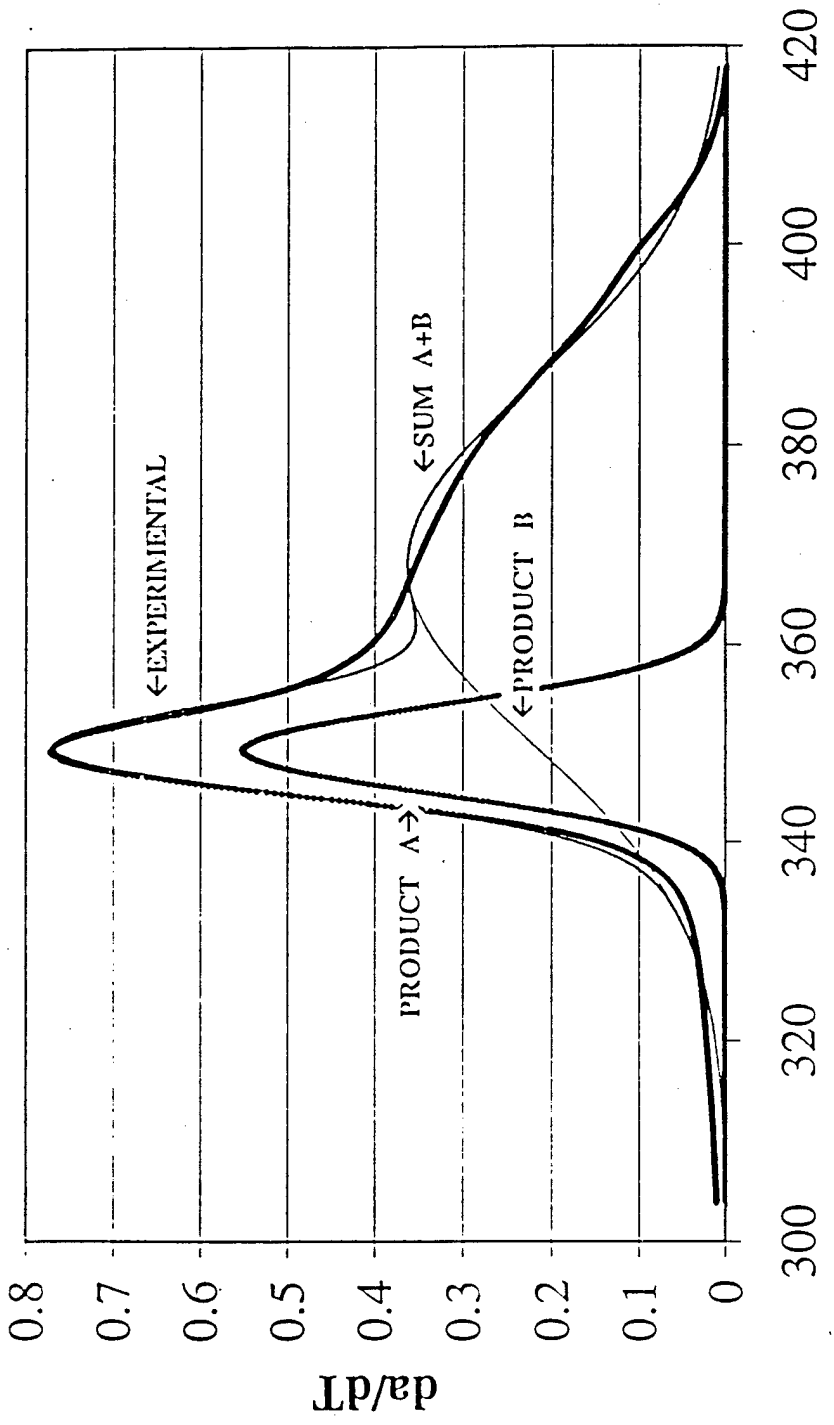

FIGURE 4 Deconvolution of the weight loss curve (Dynamic TGA: scan rate 1°/min) for the degradation of wire (irradiated 19 Mrads) in oxygen.

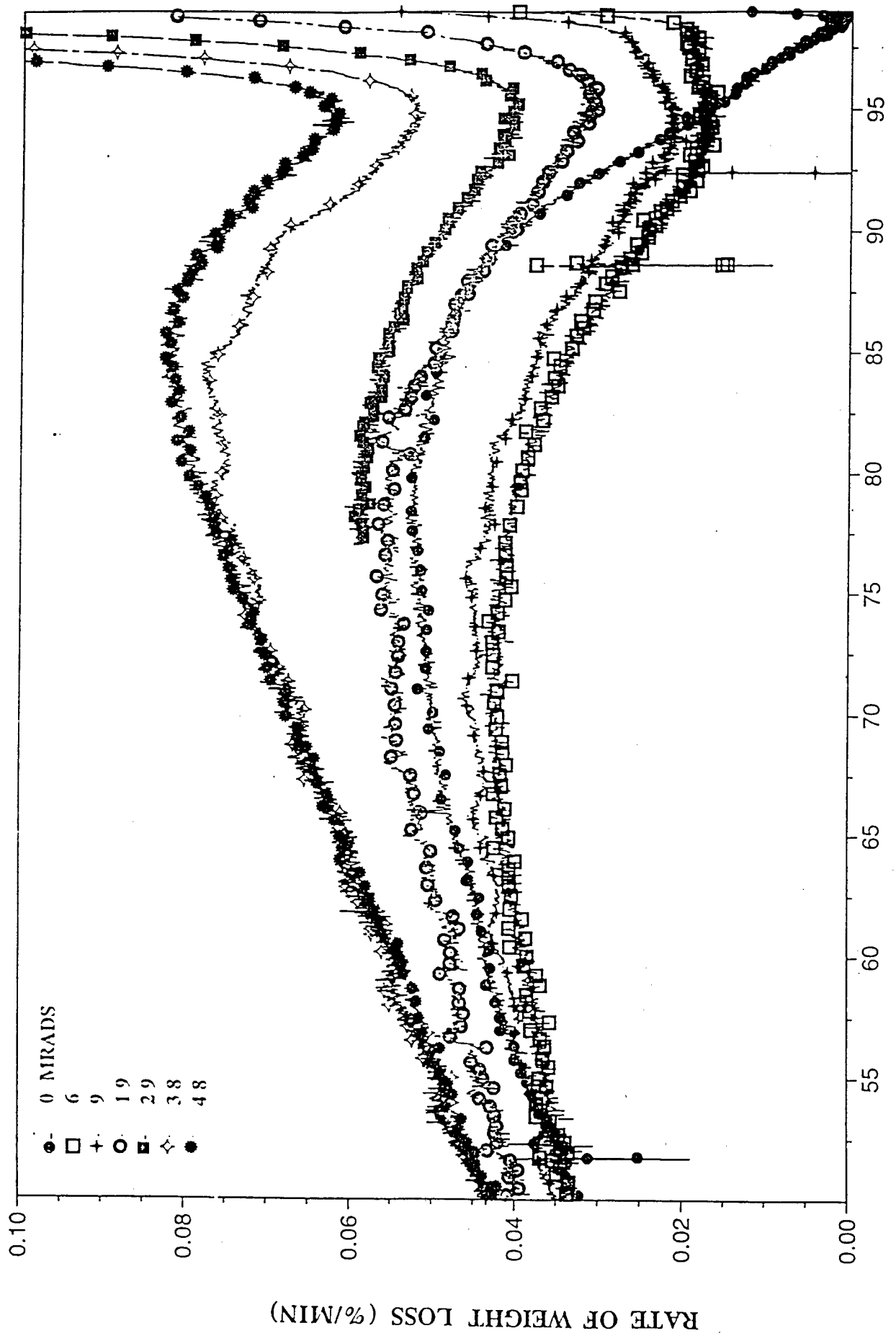

Figure 5. Rate of weight loss as a function of degree of conversion (1-α) and radiation dose for the degradation of PTFE in air

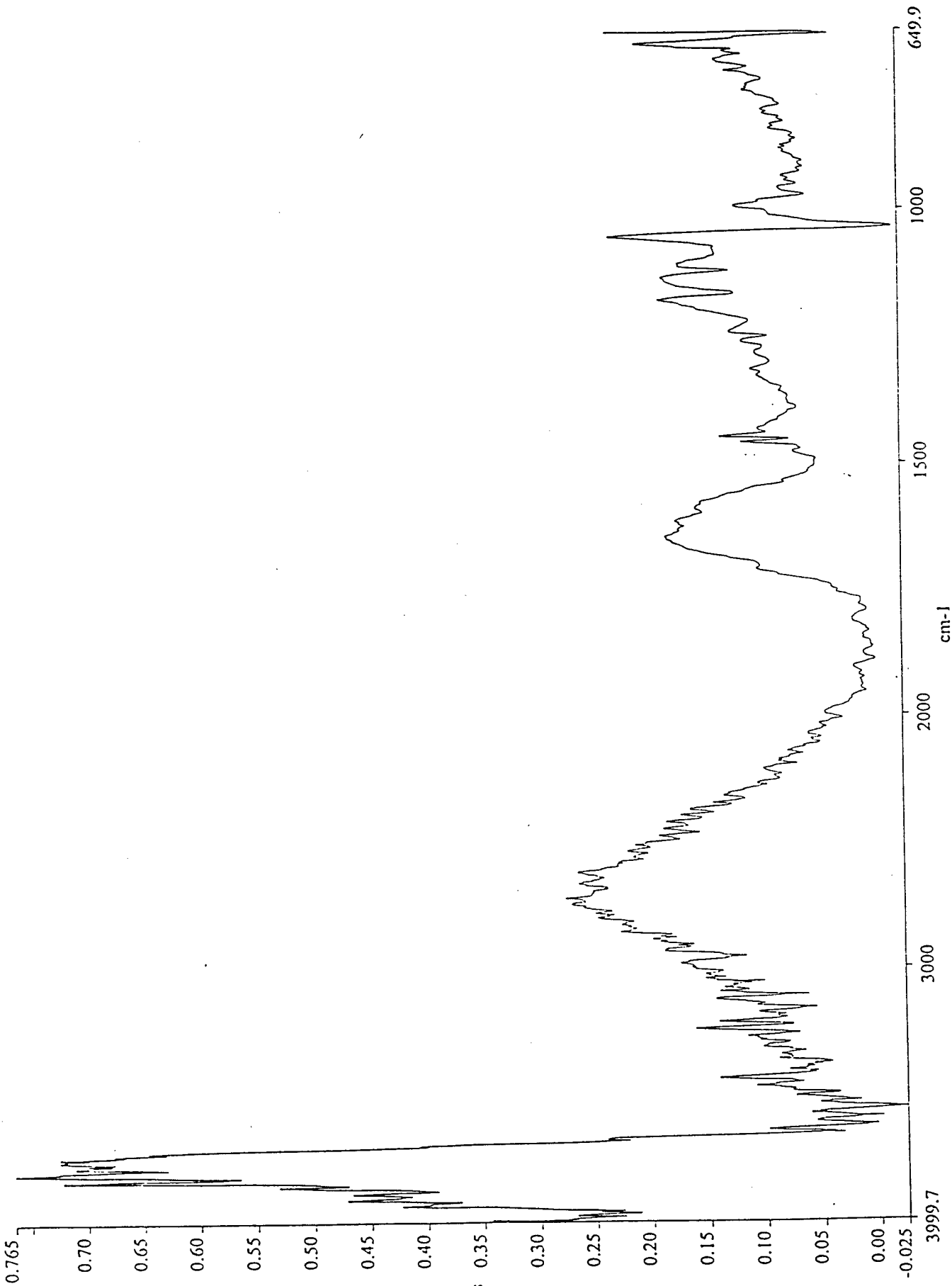

FIGURE 6. FTIR difference spectrum. Sample irradiated to 6 Mrads

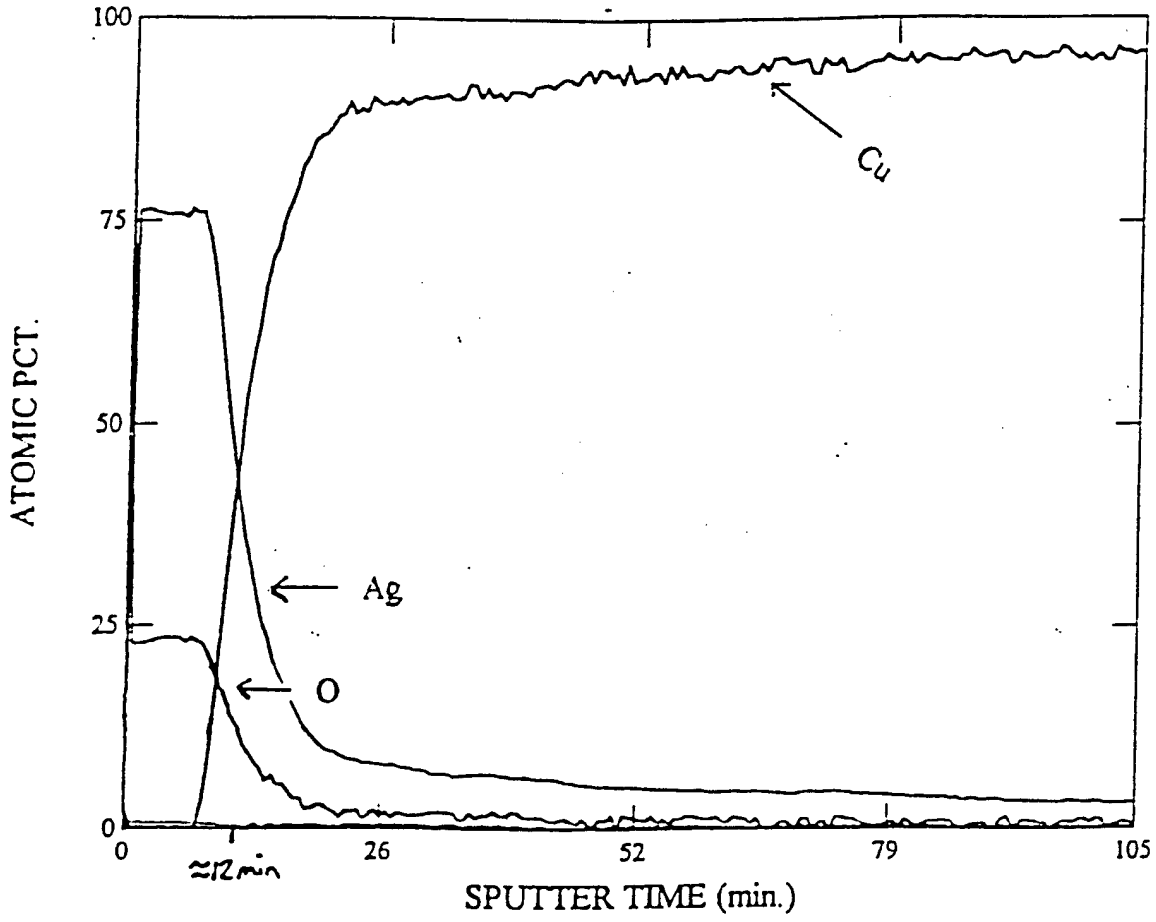

7. Auger sputter profile from an imaged sample of silver plated copper irradiated to a total dose of 48 MRads.

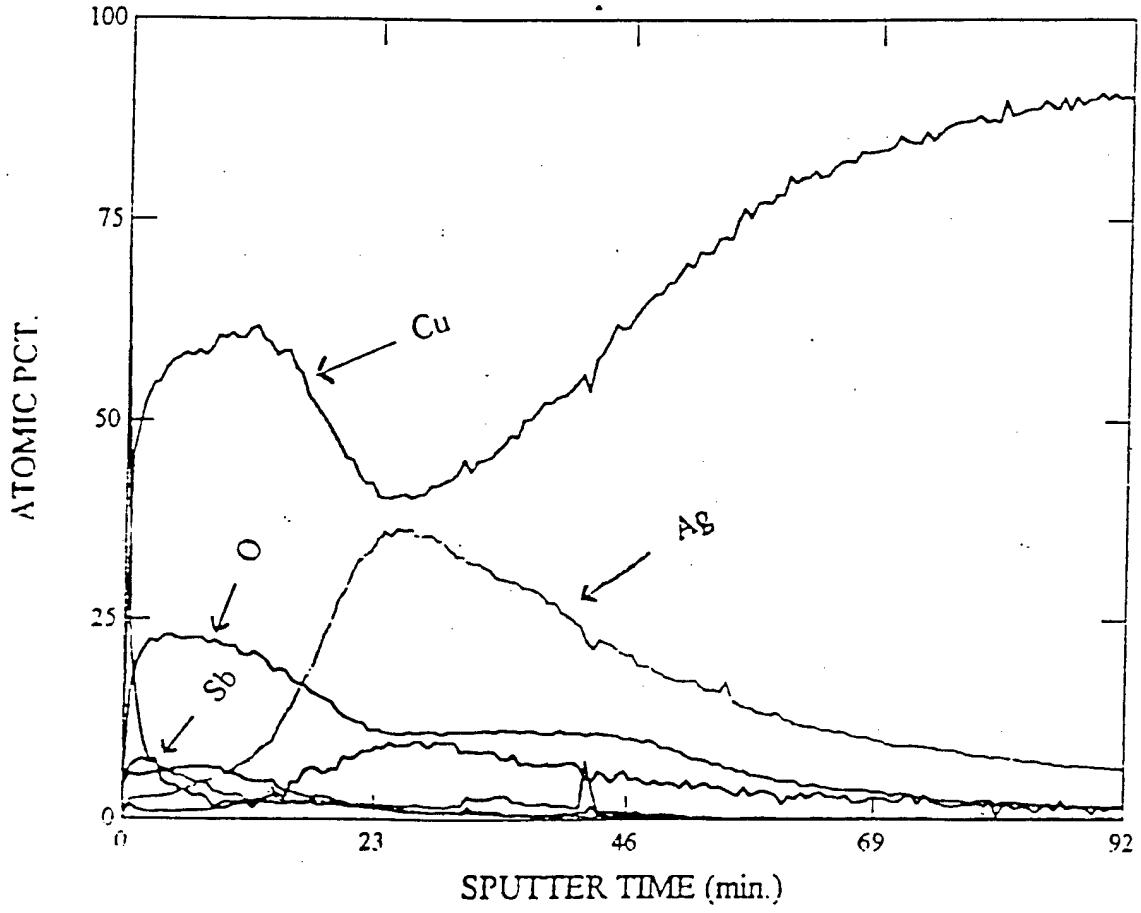

8. Auger sputter profile of a silverplated copper sample irradiated to a total dose of 48 MRads and aged at 250°C for 181 hours.

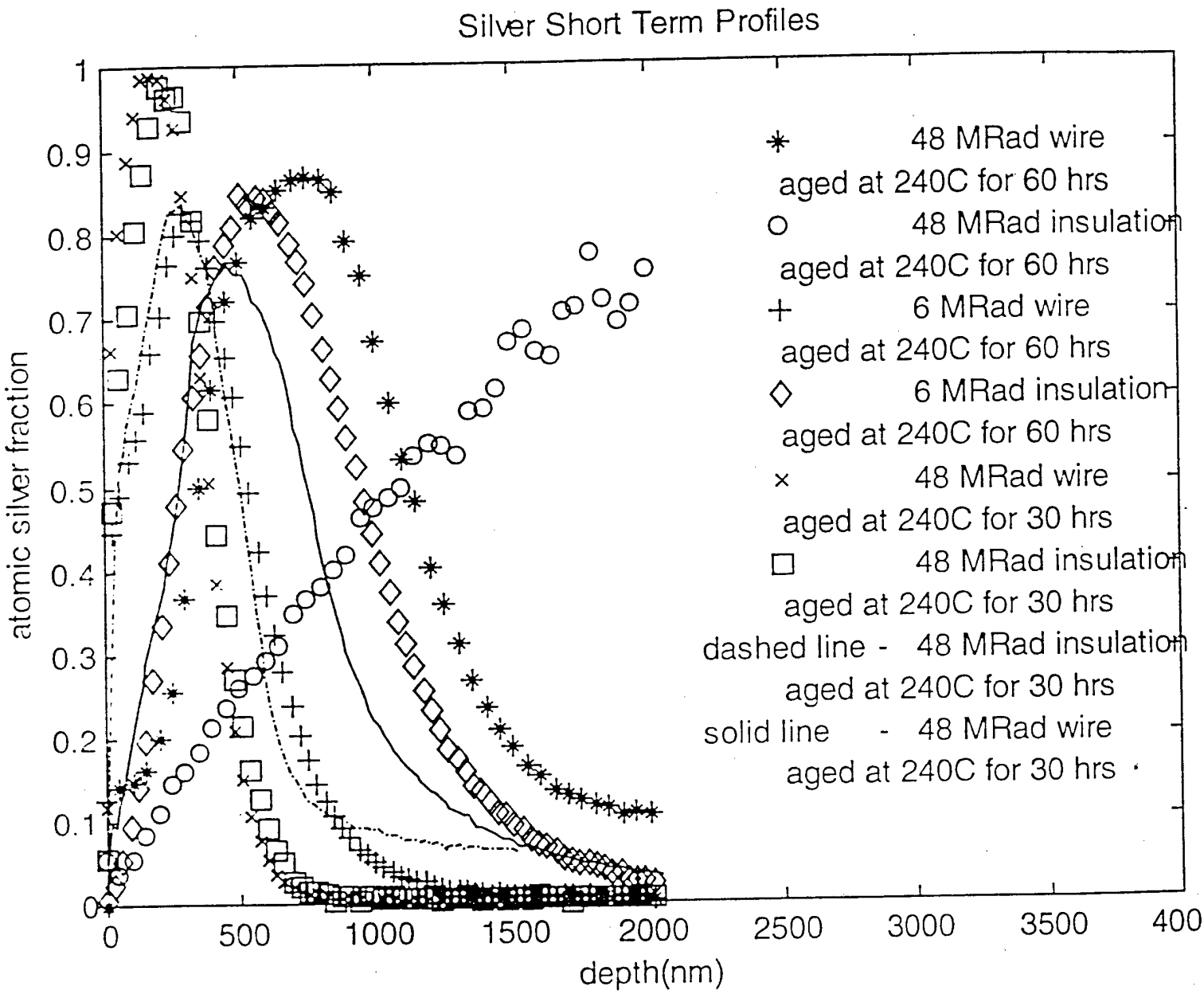

9. Comparison of auger sputter profiles from insulation and wire aged at different oxidizing conditions.

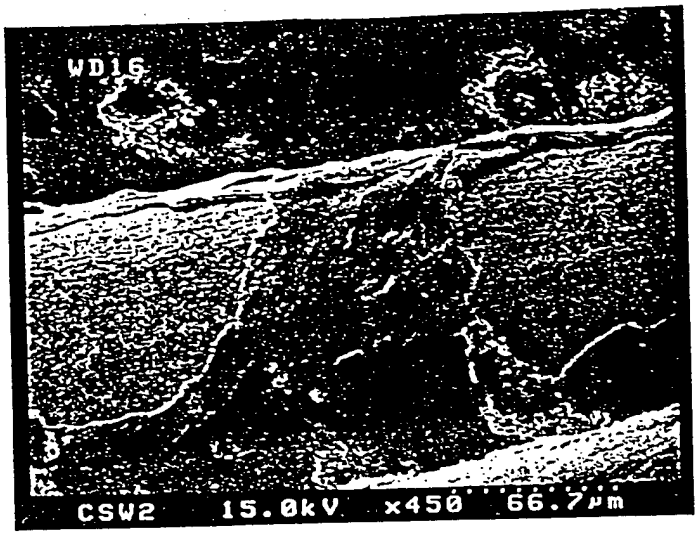

FIGURE 10. SEM photomicrograph of conductor showing silver plate debonding from copper substrate. Sample was aged with an ETFE overlay for 20 hours at 270°C.

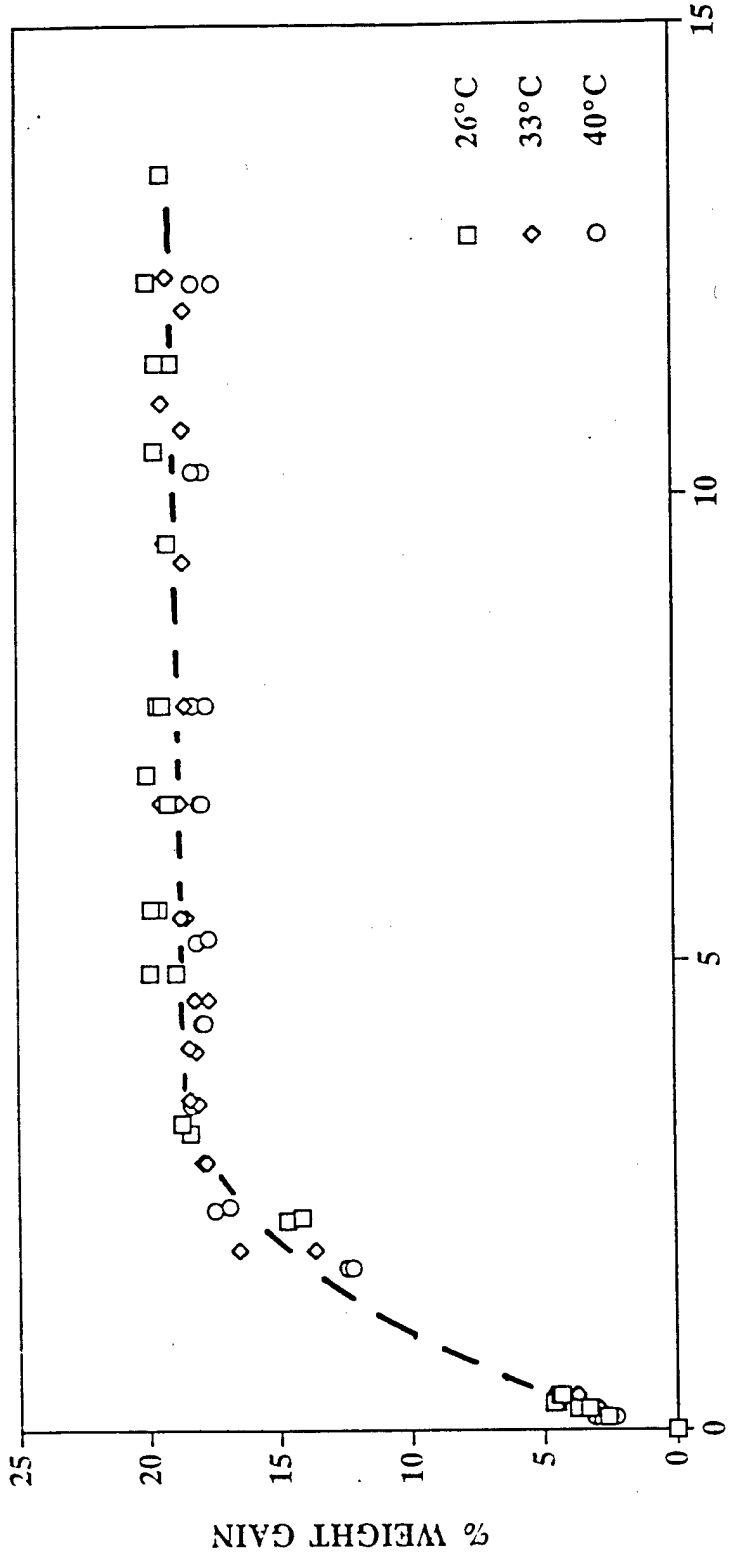

FIGURE 11. Sorption of carbon disulfide into amorphous PPS at different temperatures.

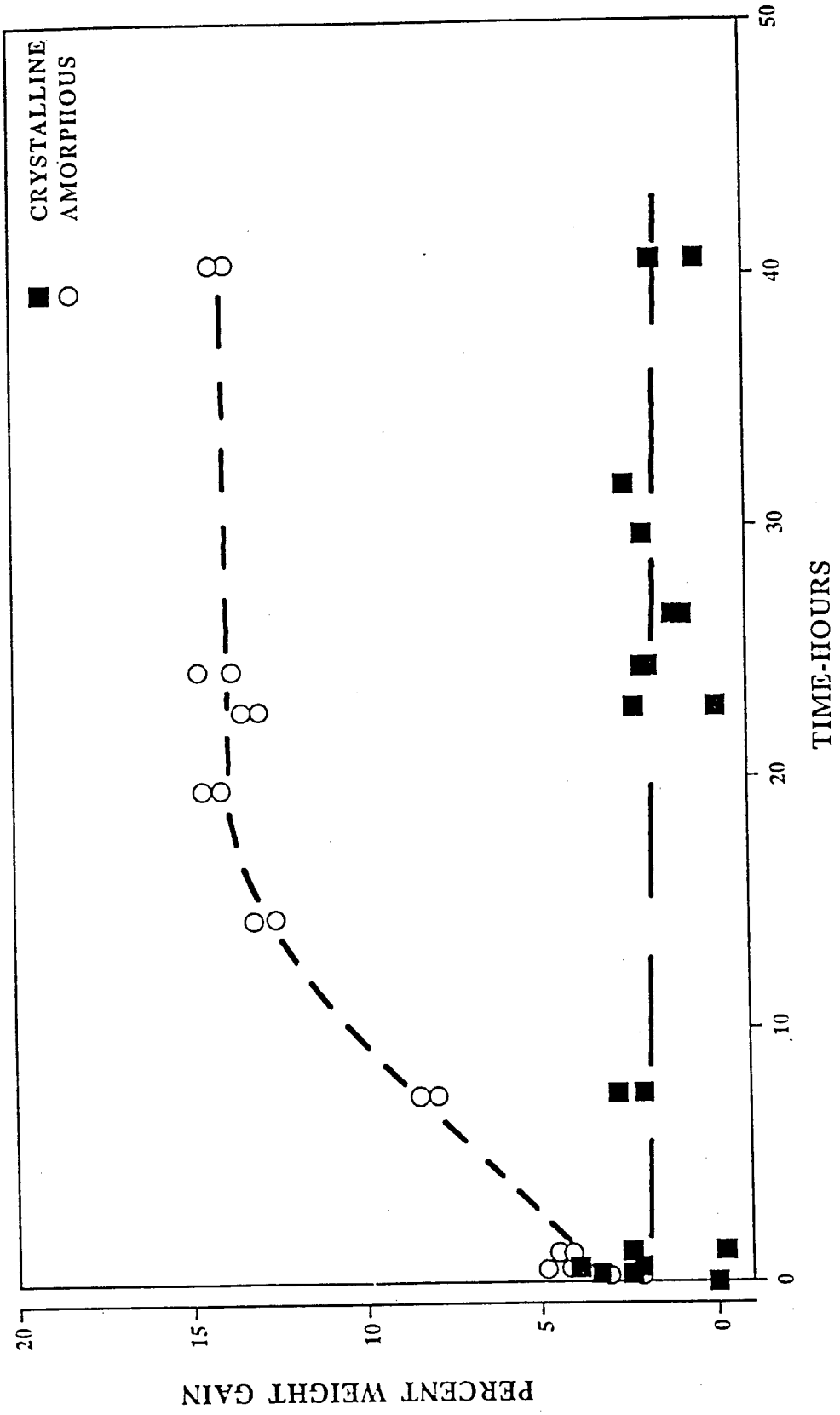

FIGURE 12. Sorption of toluene into amorphous and crystalline PPS at 24°C.

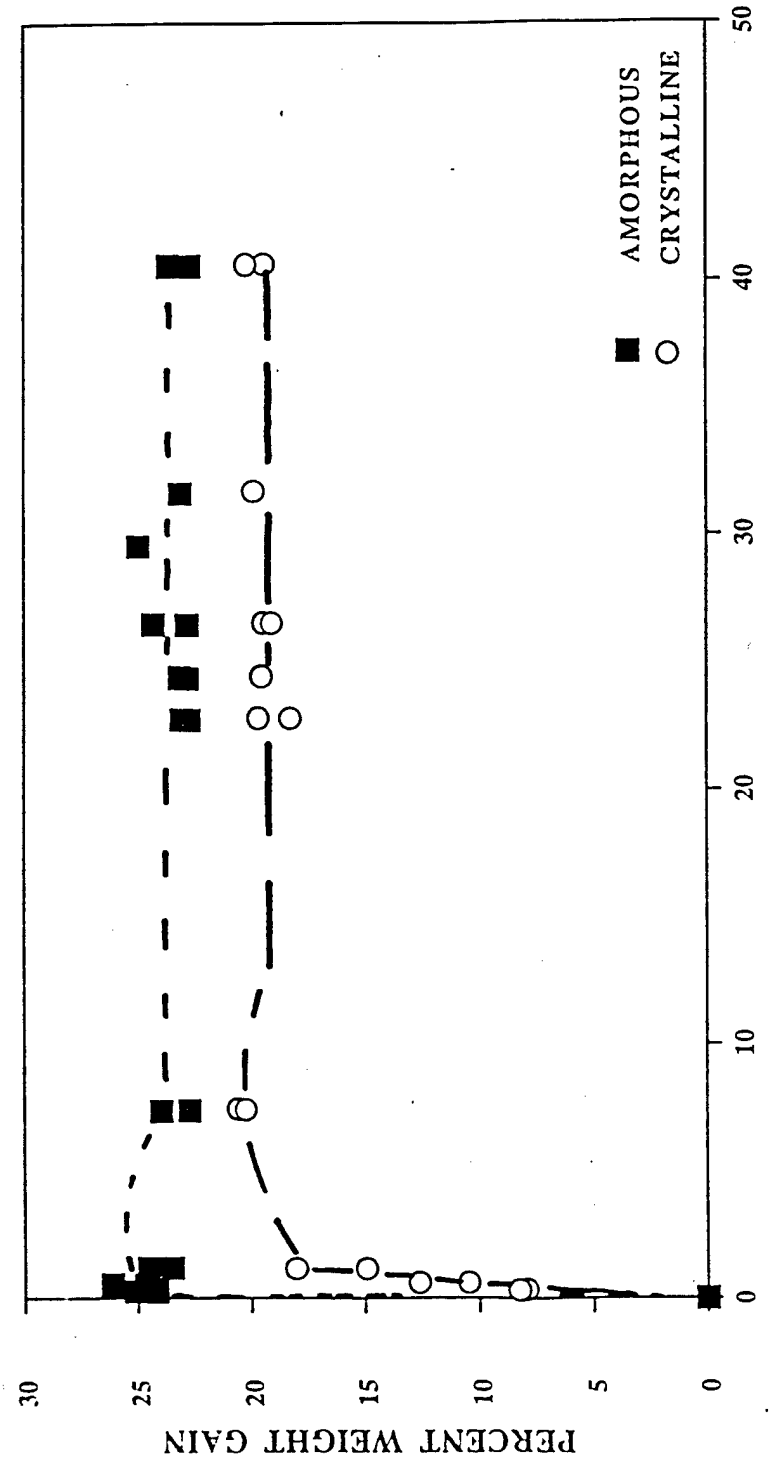

FIGURE 13. Sorption of carbon disulfide into amorphous and crystalline PPS at 24°C.

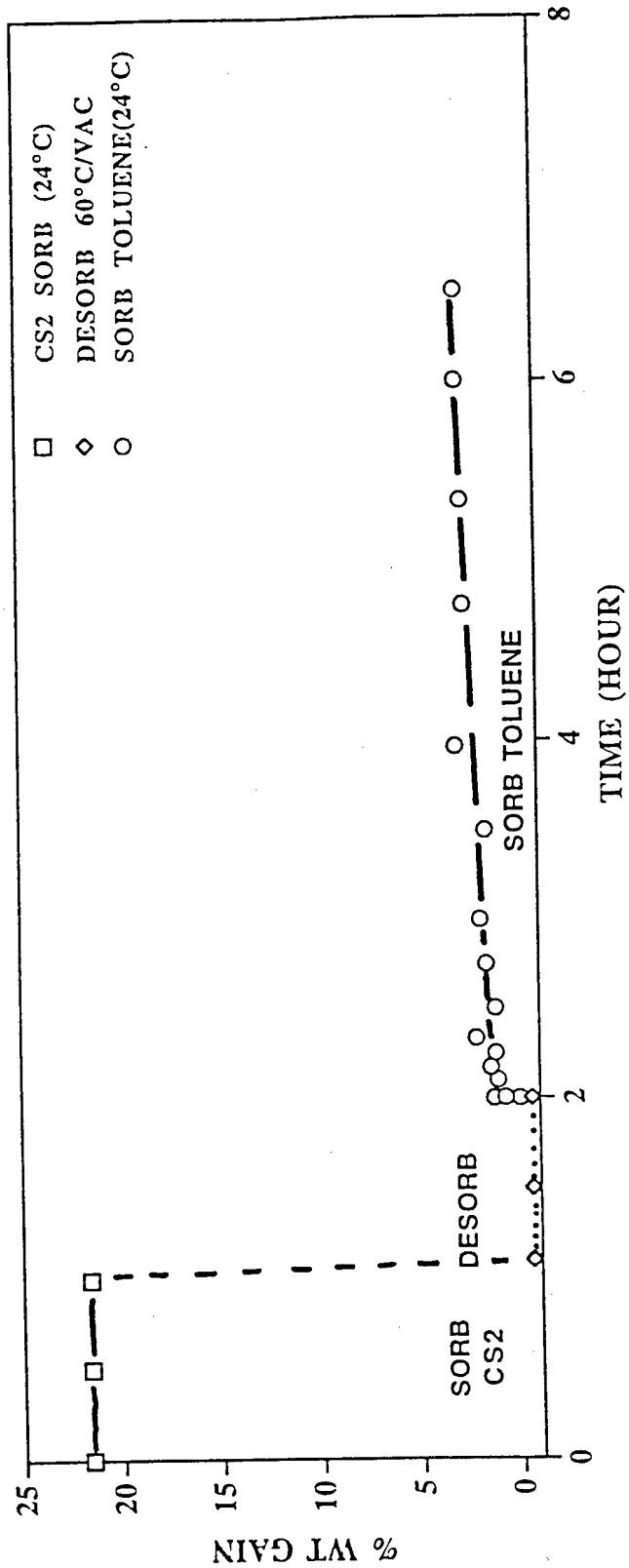

FIGURE 14. Sorption(24°C) and desorption(60°c/vacuum) of carbon disulfide into PPS followed by Resorption of toluene(24°C).

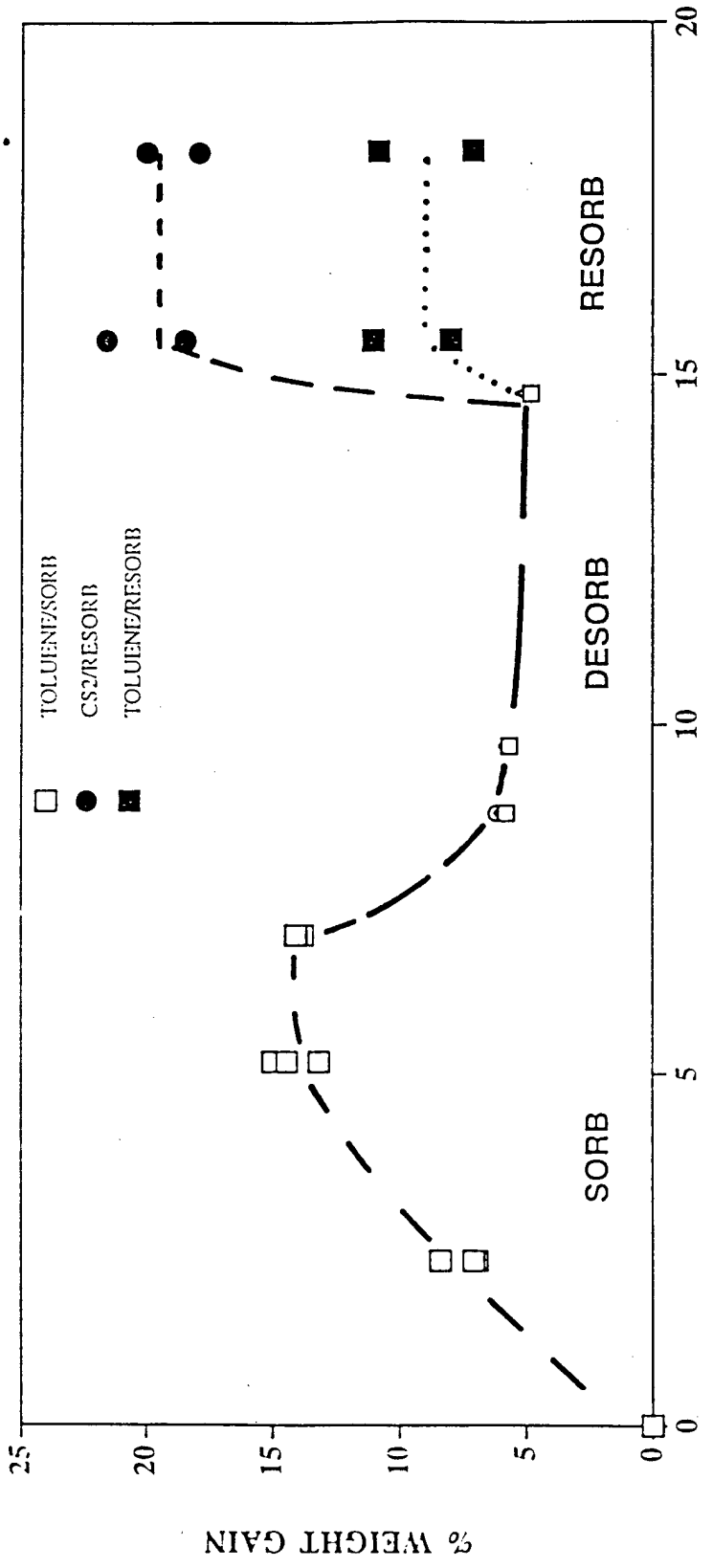

FIGURE 15. Sorption(24°C) and desorption(60°C/vacuum) of toluene into PPS followed by the sorption of toluene or carbon disulfide.

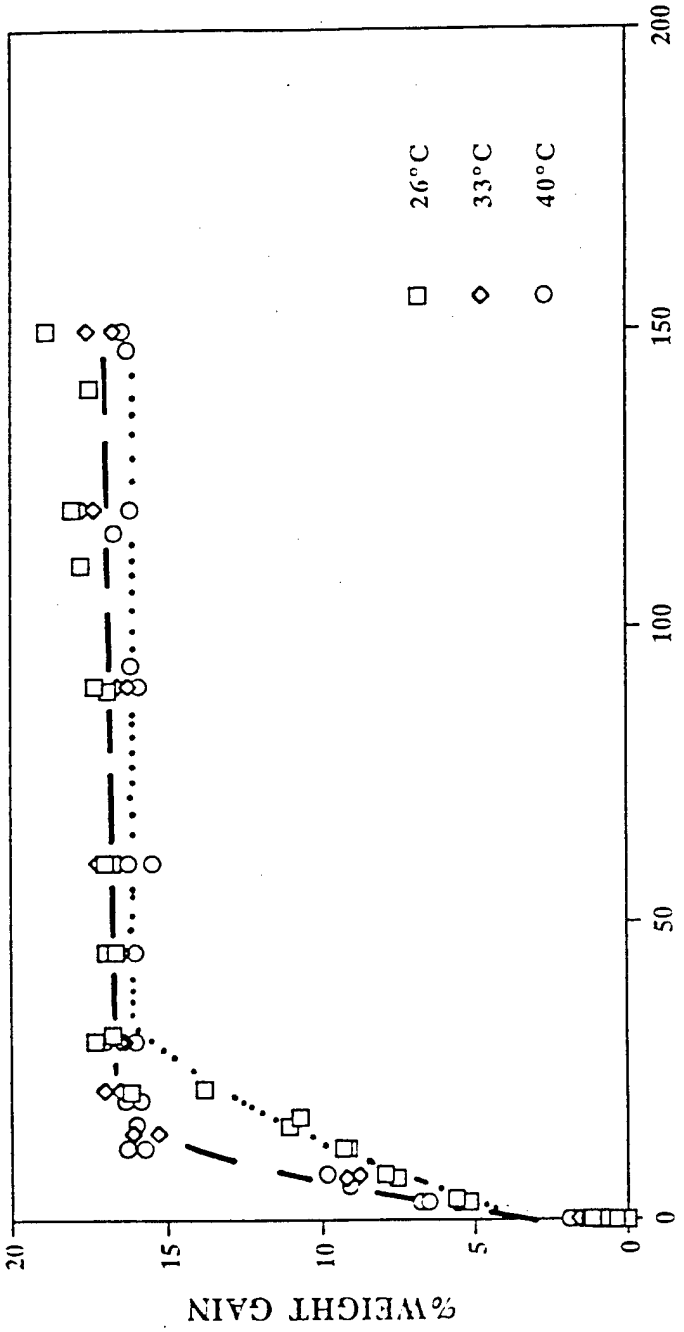

FIGURE 16. Resorption of carbon disulfide following sorption and subsequent desorption of carbon disulfide at different temperatures.

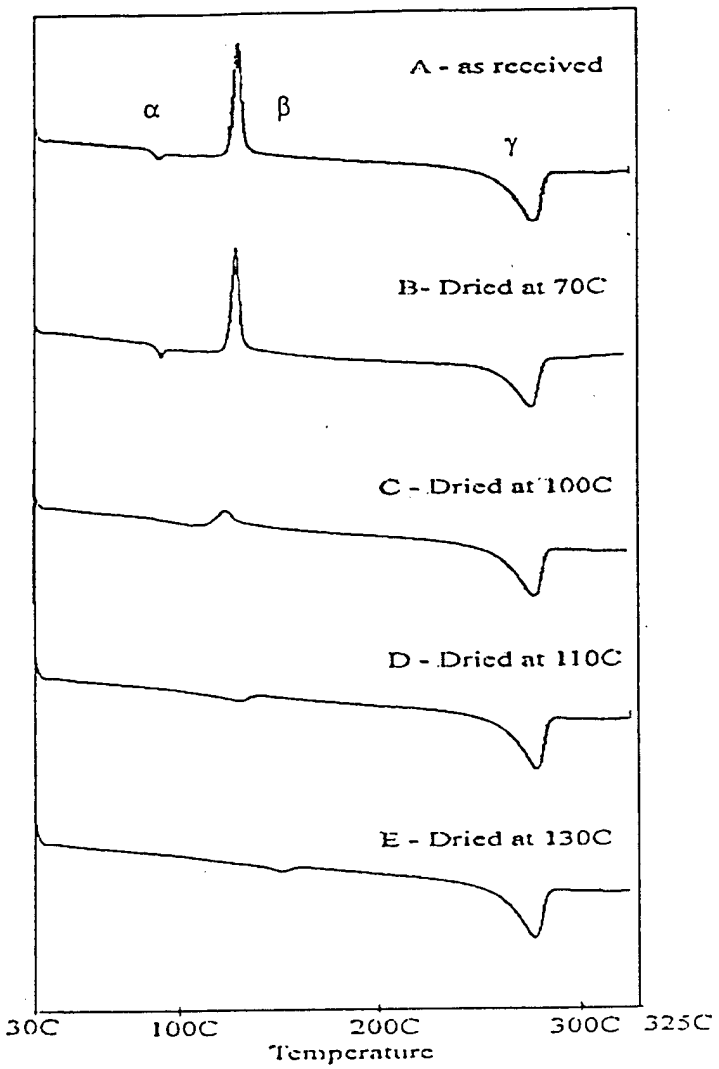

FIGURE 17. DSC thermograms from PPS annealed at different temperatures.

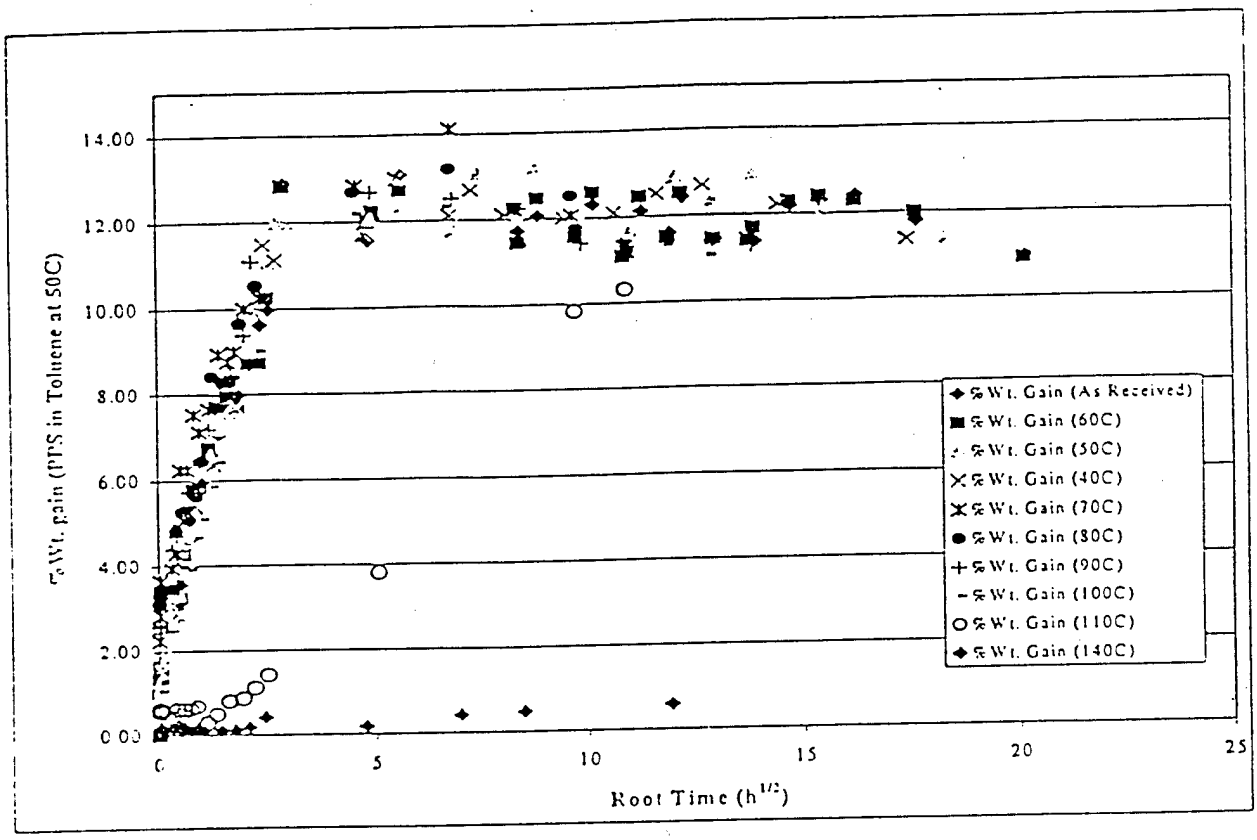

FIGURE 18. Percent weight gain of toluene into PPS following thermal anneal.

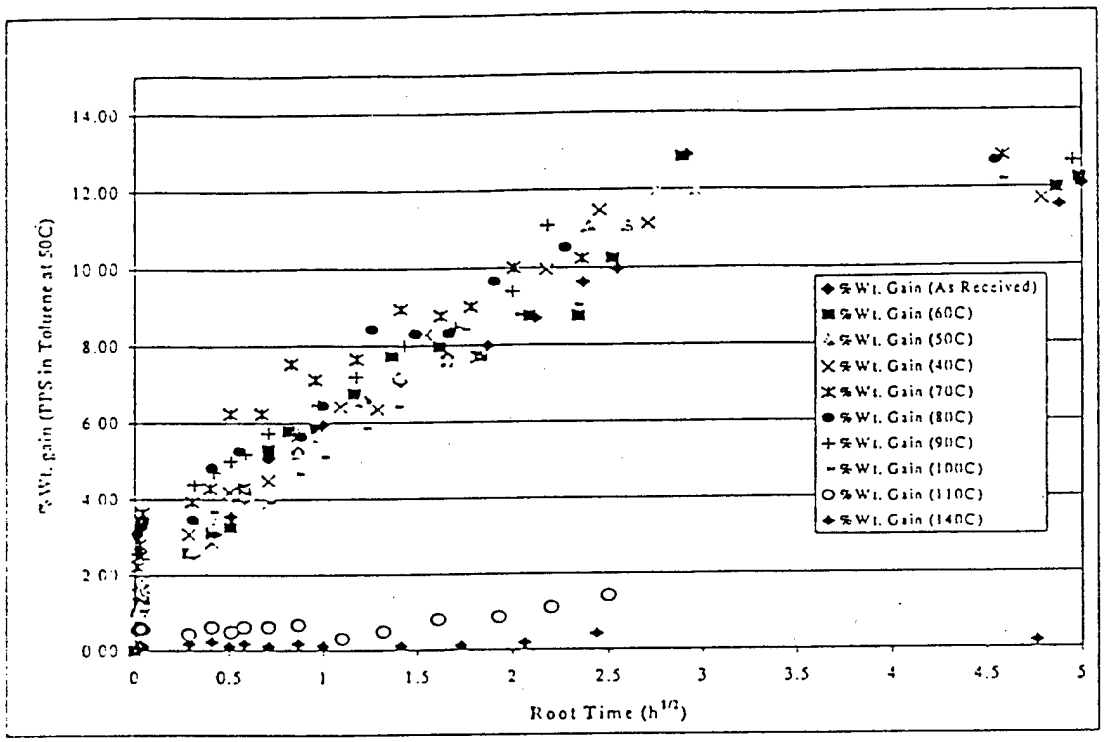

FIGURE 19. Expanded view of the weight gain curve shown in Figure 18.

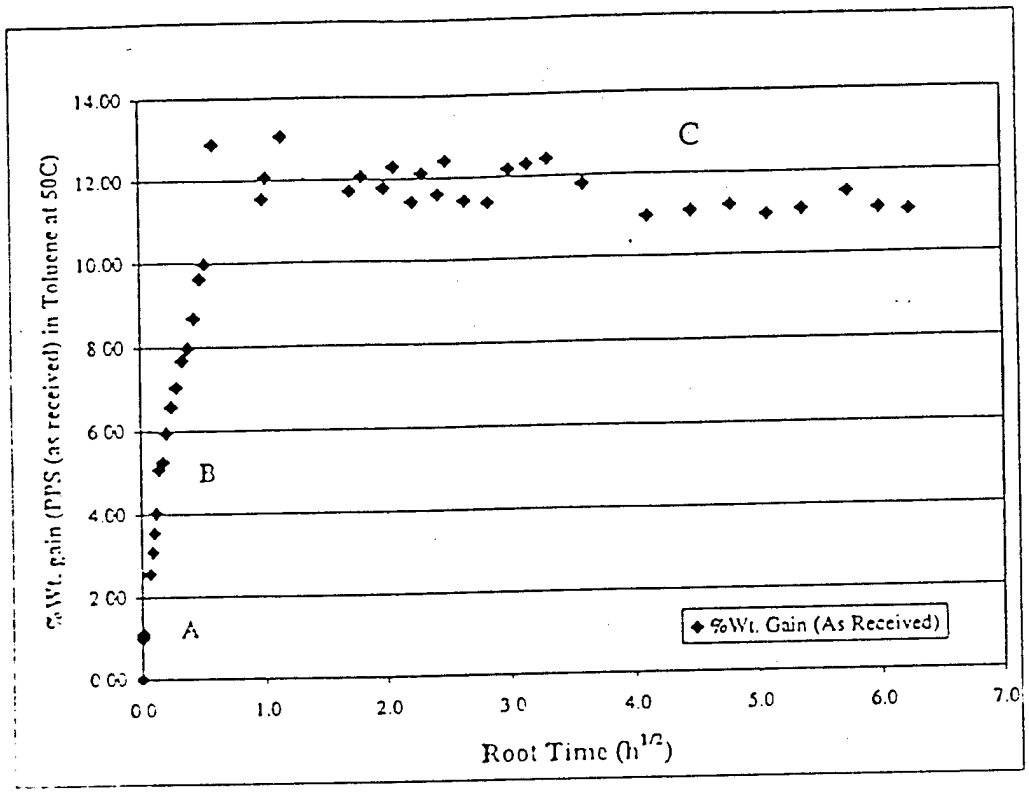

FIGURE 20. Percent weight gain curve for the sorption of toluene into amorphous PPS at 50°C.